Biosystems Engineering

Use of Computational Fluid Dynamic tools to model the coupling of plant canopy activity and climate in greenhouses and closed plant growth systems: a review.

--Manuscript Draft--

Manuscript Number:	YBENG-D-22-01328R2
Article Type:	Review Article
Keywords:	Greenhouse; Crop Model; plant; Transpiration; photosynthesis; cfd; Porous Medium; User Defined Function UDF
Corresponding Author:	Hicham Fatnassi International Center for Biosaline Agriculture UNITED ARAB EMIRATES
First Author:	Hicham Fatnassi
Order of Authors:	Hicham Fatnassi
	Pierre Emmanuel Bournet
	Thierry Boulard
	Jean Claude Roy
	Francisco D. Molina-Aiz
	Rashyd Zaaboul
Manuscript Region of Origin:	Middle East
Abstract:	Since the 1990s, CFD has allowed significant progress in the distributed climate and crop modeling in greenhouses. The quality of CFD modeling chiefly relies on its capacity to depict the dynamic interaction of the crop with airflow and the subsequent heat and mass exchanges. CFD approach combines different scales of modeling, i.e., the greenhouse and its environment with the crop canopy, with an accuracy of a few cubic centimeters. This approach accounts for the coupling of air transfers within the crop assimilated to the solid matrix of a porous medium exchanging momentum, heat, and mass with air. The sink and source terms for momentum, sensible and latent heat fluxes, and other mass exchanges are assigned to each cell of the porous medium. The local air velocity, temperature, humidity, and radiation can be calculated by solving the conservation equations together with the radiative transfer equation. The crop canopy's CO2 and evapotranspiration distributions are deduced from the locally distributed climate. In this paper, the coupling of the plant activity with its local microclimate using the CFD modeling approach is described in detail. Its implementation through a User Defined Function (UDF) coupling the crop submodel to the main CFD solver is also provided. The primary studies related to the CFD modeling of crops inside greenhouses are reviewed concerning various interactions such as loss of momentum, transpiration, photosynthesis, and the characteristics of the field experiments used for validations. From this analysis, future trends of CFD developments applied to crop activity are also presented.
Suggested Reviewers:	In-Bok Lee, Professor Seoul National University iblee@snu.ac.kr
	Murat Kacira, Professor The University of Arizona mkacira@email.arizona.edu
Opposed Reviewers:	
Response to Reviewers:	

CONFLICT OF INTEREST

Manuscript title: Use of Computational Fluid Dynamic tools to model the coupling of plant canopy activity and climate in greenhouses and closed plant growth systems: a review.

The authors whose names are listed immediately below certify that they have NO affiliations with or involvement in any organization or entity with any financial interest (such as honoraria; educational grants; participation in speakers' bureaus; membership, employment, consultancies, stock ownership, or other equity interest; and expert testimony or patent-licensing arrangements), or non-financial interest (such as personal or professional relationships, affiliations, knowledge or beliefs) in the subject matter or materials discussed in this manuscript.

Author names:

Hicham Fatnassi

Pierre Emmanuel Bournet

Thierry Boulard

Jean Claude Roy

Francisco D. Molina-Aiz

Rashyd Zaaboul1,6

- Mechanical and heat and mass transfers at crop level in CFD modelling
- Radiative transfers within the crop rows in CFD modelling
- Photosynthetic activity, leaf temperature and crop transpiration in CFD modelling
- Simulation of shortwave radiation inside the crop
- Simulation of the distribution of CO_2 concentration in the greenhouse

Use of Computational Fluid Dynamic tools to model the coupling of plant canopy activity and climate in greenhouses and closed plant growth systems: a review.

Hicham Fatnassi[1,2*], Pierre Emmanuel Bournet[3], Thierry Boulard[4], Jean Claude Roy[5], Francisco D. Molina-Aiz[6] , Rashyd Zaaboul[1,6]

[1] International Center for Biosaline Agriculture, ICBA, Dubai, P.O. Box 14660, United Arab Emirates

[2] INRA, Univ. Nice Sophia Antipolis, CNRS, UMR 1355-7254 Institut Sophia Agrobiotech, 06900 Sophia Antipolis, France

[3] a, SFR 4207 QuaSaV, 49000, Angers, France

[4] 33, Avenue Saint Laurent, 06520, Magagnosc, France.

[5] FEMTO-ST, Franche-Comté University, Belfort, France.

[6] Departamento de Ingeniería Rural, Universidad de Almería, Escuela Politécnica Superior, Ctra. Sacramento, 04120 Almería, Spain

Corresponding author e-mail: h.fatnassi@biosaline.org.ae

Abstract

Since the 1990s, Computational Fluid Dynamics (CFD) has allowed significant progress in the distributed climate and crop modelling in greenhouses. The quality of CFD modelling chiefly relies on its capacity to depict the dynamic interaction of the crop with airflow and the subsequent heat and mass exchanges. CFD approach combines different scales of modelling, i.e., the greenhouse and its environment with the crop canopy, with an accuracy of a few cubic centimetres corresponding to the volume of one mesh cell in the greenhouse. This modelling approach accounts for the coupling of air transfers within the crop simulated to the solid matrix of a porous medium exchanging momentum, heat, and mass with air. The sink and source terms for momentum, sensible and latent heat fluxes, and other mass exchanges are assigned to each cell of the porous medium (i.e., canopy).

The local air velocity, temperature, humidity, and radiation distributions can then be calculated by solving the conservation equations together with the radiative transfer equation. The crop canopy's CO2 distributions and other plant activity parameters (such as evapotranspiration or photosynthesis) are deduced from the locally distributed climate. In this paper, the coupling of the plant activity with its local microclimate using the CFD modelling approach is described in detail. Its implementation through a User Defined Function (UDF) coupling the crop submodel to the main CFD solver is also provided. The primary studies related to the CFD modelling of crops inside greenhouses are reviewed concerning various interactions such as loss of momentum, transpiration, photosynthesis, and the characteristics of the field experiments used for validations. From this analysis, future trends of CFD developments applied to crop activity are also presented.

Keywords: Greenhouse, Crop Model, Plant, Transpiration, Photosynthesis, CFD, Porous Medium, User Defined Function UDF

Nomenclature

a_1	Empirically determined parameter
a_2	Empirically determined parameter
a_3	Empirically determined parameter
b_1	Empirically determined parameter
b_2	Empirically determined parameter
b_3	Empirically determined parameter
C	Sensible heat flux density, in W m^{-3}
C_a	Concentration of CO_2
C_D	Drag coefficient
C_F	Non-linear momentum loss coefficient
C_p	Specific heat at constant pressure, in J kg^{-1} K^{-1}
d	Characteristic dimension of the leaves, in m
dV	Volume element, in m^3
E	Evaporated water flux, in kg m^{-3} s^{-1}
Gr	Grashof number
h_s	Heat exchange coefficient, in W m^{-2} K^{-1}
H	Average height of the crop row, in m
I	PAR incident radiative flux, in W m^{-2}
K	Permeability of the porous medium, in m^2
K_C	Radiation extinction coefficient
L	Length of the crop row, in m
l	Width of the crop row, in m
LAD	Leaf area density, in m^2 m^{-3}
LAI	Leaf area index, in m^2 m^{-2}
L_v	Heat of vaporisation of water, in J kg^{-1}
Nu	Nusselt number
P_r	Photosynthesis flux, in kg_{CO2} m^{-3} s^{-1}
Prt	Prandtl number
q_l	Latent heat flux density, in W m^{-3}

q_s	Convective sensible heat flux density, in W m^{-3}
R_{abs}	Net radiation intercepted by plant leaves, in W m^{-3}
Rg_0	Global radiation intercepted at the top of the crop cover, in W m^{-2}
$Rg(z)$	Global radiation along the optical path of the sun at a distance z from the top of the canopy, in W m^{-2}
r_a	Aerodynamic resistance, in s m^{-1}.
Re	Reynolds number
r_s	Stomatal resistance, in s m^{-1}
r_t	Total resistance, in s m^{-1}
S_{CO2}	Net photosynthesis consumption flux, in kg_{CO2} m^{-3} s^{-1}
$S_\emptyset$	Source term
T_a	Air temperature, in K
T_l	Leaf temperature, in K
T_{max}	Empirically determined parameter, in K
U	Component of the velocity vector according to X-axis, in m s^{-1}
v	Air speed within the crop cover, in m s^{-1}
V	Component of the velocity vector according to Y-axis, in m s^{-1}
VPD_a	Air-air vapor pressure deficit, in Pa
VPD_0	Empirically determined parameter, in Pa
W	Component of the velocity vector according to Z-axis, in m s^{-1}
w_a	Absolute humidity of the surrounding air, in kg kg^{-1}
w_l	Absolute saturating humidity at the leaf level, in kg kg^{-1}
z	Distance from the top of the canopy, in m
Φ	Concentration of the transported quantity,
μ	Dynamic viscosity of air, in kg m^{-1} s^{-1}
Γ	Diffusion coefficient, in Kg m^{-1} s^{-1}
γ	Psychrometric constant, in Pa K^{-1}
Δ	Slope of the saturated water vapor pressure curve, in Pa K^{-1}
τ	Leaf conductance, in m s^{-1}
ρ	Air density, in kg m^{-3}

α Photosynthesis efficiency, in $kg_{CO2}\ J^{-1}$

λ_a Air conductivity, in $W\ m^{-1}\ K^{-1}$

Subscripts

a refers to air

C refers to CO_2

l refers to leaf

w refers to H_2O

Abbreviation

CFD Computational Fluid Dynamics

DO Discrete ordinates model

LAD Leaf area density

LAI Leaf area index

LWD Leaf Wet Duration

RTE Radiative transfer equation

UDF User-Defined Function

1. Introduction

Computational Fluid Dynamics is a branch of fluid mechanics that uses numerical analysis and data structures to solve problems that involve fluid flows. It allows simulating the distribution of fluid flow variables inside a calculation domain. Considering the words "Computational Fluid Dynamics", on the Scopus™ database it was found that more than 90 000 CFD papers were published during the 1974 – 2021 period reaching around 9000 papers in 2021. Engineering represented more than 30% of CFD publications, followed by physics and astrophysics, chemical engineering, energy, mathematics, material science, computer sciences and environmental sciences.

The application of CFD in agriculture area has grown significantly since the end of the 90s (Norton et al., 2007). The first CFD studies in greenhouses were devoted to ventilation issues and design optimisation without considering the activity of the crop (Okushima et al., 1989; Mistriotis et al., 1997 a, b and c). Recent and important progress was observed in the modelling of the greenhouse distributed climate and particularly the climate at crop level, by including the effect of the dynamic action of the crop on the flow and the subsequent heat and mass transfers (Haxaire,1999; Boulard and Wang, 2002; Fatnassi et al., 2003, 2006, 2015; Majdoubi et al., 2009; Kichah et al., 2012; Tamimi et al., 2013; Majdoubi et al., 2016; Boulard et al., 2017; Tadj et al., 2017; Bouhoun Ali et al., 2018; Bouhoun Ali et al., 2019; Baxevanou et al., 2020; Ben Amara et al., 2021; Cheng et al., 2021; Liu et al., 2021; An et al., 2022).

1.1. Dynamic, heat and mass transfers at crop level

Haxaire (1999) was, to our knowledge, the first to integrate the drag and transpiration effects of plant canopies in the airflow inside the greenhouses by customising a CFD commercial software CFD2000®, (CFD2000, 1997) by means of source terms. He

previously conducted wind tunnel tests to determine the relationship between the crop leaf area index and the pressure drop produced for different air velocities, calculating the value of the drag coefficient of a tomato plant canopy. The concept of simulating crop rows inside a greenhouse using a "porous medium" was first introduced by Haxaire (1999). Due to the complex geometry of real crop rows in a greenhouse, which demands a powerful computer and is time-consuming, he opted to model crop rows as parallelepiped-shaped porous media. This approach consists of a solid matrix (representing the plants) with interconnected pores (representing air). Boulard and Wang (2002) carried out CFD simulations of a lettuce crop transpiration inside a plastic tunnel including both global solar radiation transfers and crop heat exchanges while Roy and Boulard (2003) predicted natural ventilation and climate in a tunnel-type greenhouse using the same crop submodel adapted to tomato and considering the crop as a porous medium. For tomato plants, they simulated each mesh of the crop subdomain to volumetric heat and water vapor sources. The radiative flux was partitioned into convective sensible and latent heat fluxes (depending on the stomatal and aerodynamic resistances) inside a virtual solid matrix of the porous medium. This matrix representing the crop was characterised by its leaf temperature and its drag coefficient (Haxaire, 1999; Boulard and Wang, 2002; Boulard et al., 2002).

Fatnassi et al. (2003) adapted the CFD code to simulate the sensible and latent heat exchanges of tomato plants in a large-scale Canarian greenhouse, and later in a multispan plastic greenhouse equipped with insect-proof screens (Fatnassi et al. 2006). Similarly, Liu et al. (2021) and An et al. (2022) customised the CFD code to model cucumber and tomato transpiration and condensation on leaves in Chinese Solar Greenhouses (CSG), using a similar approach.

168 **1.2. Photosynthetic activity**

169 CFD modelling also focused on photosynthesis, which is another important parameter of
170 plant activity. Reichrath et al. (2001) developed a CFD model of a large commercial Venlo-
171 type glasshouse that included the crop as a carbon dioxide sink, following the formulation
172 proposed by Acock et al. (1978). In their studies, the uptake of CO_2 for photosynthetic
173 activity was assumed to be proportional to the CO_2 concentration and leaf area index (Hand,
174 1973).

175 There was apparently no further development on this topic until Roy et al. (2014) and
176 Boulard et al. (2017) implemented a CFD model to simulate photosynthesis. They
177 simulated the transpiration rate in a closed greenhouse together with the leaf gross
178 photosynthesis flux as a function of the CO_2 concentration and incident photosynthetically
179 active radiation from the model proposed by Thornley (1976) and the calculated
180 transpiration and photosynthesis rates were then compared with experimental results based
181 on direct measurements.

182 More recently Molina et al. (2017) developed a CFD model to simulate photosynthesis in
183 an Almeria-type greenhouse by incorporating the Acock‘s model.

184 **1.3. Validation of the greenhouse-crop model**

185 The combination of numerical modelling and climate characterisation studies has allowed
186 the validation of these numerical greenhouse-crop models for air temperature, humidity, air
187 velocity, and ventilation rate in multispan plastic-houses (Haxaire, 1999; Fatnassi et al.,
188 2006), large greenhouse-tunnels (Boulard and Wang, 2002; Nebbali et al., 2012) large scale
189 Canarian type plastic-houses (Fatnassi et al., 2003; Majdoubi et al., 2009), single span
190 greenhouses (Bartzanas et al., 2002), Venlo-type closed greenhouse equipped with air
191 conditioners (Boulard et al., 2017) and Chinese Solar Greenhouses (CSG) (Wang et al.,

2013; Zhang et al., 2016; Tong et al., 2018; Jiao et al., 2020; Liu et al., 2021; Xiaoyang et al., 2021; An et al., 2022). The realism of the results and the good fit which were generally observed between measured and simulated values of the climate fields in all these studies give confidence in the use of these coupled microclimate-crop numerical models .

1.4. Improving the canopy representation in CFD crop models

As previously reviewed, the canopy considered as a "porous medium" is one of the main phenomenological approaches of the physical transfers within the crop cover, however, it is not the only one and plant-CFD modelling can be based on approaches which try to consider the exact form of leaves and plants, even of stomata. Thus, a numerical model based on the energy balance has been combined with the Fluent CFD code for computing temperature and humidity at leaf surface for single bean leaves at low light levels (Roy et al., 2008). Defraeye et al. (2014) developed an innovative three-dimensional CFD cross-scale modelling approach to investigate convective mass transport from leaves. Notably, they bridged the gap between stomatal and leaf scale by including all these scales in the same computational model, which implies explicitly modelling individual stomata. More recently, Yu et al. (2022) numerically investigated the effects of natural light and ventilation on a 3D tomato body climate distribution in a Venlo greenhouse with CFD. The 3D tomato model built based on SolidWorks allows to set up with realism the radiative and convective (sensible) transfers, however plant transpiration was not considered in the model.

1.5. Scope of the present paper

Based on this literature review, previous studies reveal that the equivalent porous medium approach can cover successfully all the bio-physical transfers implied in the plant-climate

interactions. For that reason, this paper focuses on CFD crop submodels using the porous medium concept and shows how to implement heat, and mass exchanges in such models. As the studied numerical model is composed of two sub models i.e., physical and ecophysiological, that form two loops exchanging data, an overall description of the CFD model will be first presented before the different steps of including the various heat and mass exchanges between the plant and its environment are listed. A detailed description of how to implement crop interactions with local environment in the CFD modelling follows, as well as the instructions to calculate the corresponding fluxes in the computer language, are given. Finally, the main results obtained from CFD simulations using a crop submodel are summarised and discussed.

2. Description of the CFD numerical model

2.1. Fundamentals of CFD applied to greenhouses

The CFD modelling approach of the greenhouse system is based on the combination of fluxes in different elements of a 3D domain i.e., the greenhouse and its immediate environment, together with the equipment and crop inside the greenhouse itself, the crop being simulated to a porous medium that exchanges heat and water vapor with the ambient environment (Fatnassi et al., 2003; Fatnassi et al., 2006). This model has been adapted from Haxaire (1999) and Boulard & Wang (2002) to evaluate the airflow, temperature, and humidity patterns in a real size greenhouse.

CFD is based on the solution of a set of equations for the mass, momentum, and energy conservation:

$$\frac{\partial(U\Phi)}{\partial X} + \frac{\partial(V\Phi)}{\partial Y} + \frac{\partial(W\Phi)}{\partial Z} = \Gamma.\nabla^2\Phi + S_\Phi \quad (1)$$

where Φ represents the concentration of the transported quantity, namely the scalar mass fraction, the three-dimensional velocity components (Navier-Stokes) and the temperature; U, V and W are the components of the velocity vector; Γ is the diffusion coefficient; and $S_{\emptyset}$ is the source term.

Advanced computational fluid mechanics software (such as CFD2000 ©, (CFD2000, 1997) or Ansys Fluent ©, (Ansys, 2010)) was used by most authors in the last two decades to solve these highly non-linear equations using a spatial finite volume discretisation. Two main discretisation methods are used in naturally ventilated greenhouses, one is based on the Finite Element Method (FEM) and the second one on the Finite Volume Method (FVM). FVM software (mainly ANSYS/FLUENT v 6.3.) is the most frequently used. Molina et al. (2010) conducted a specific study to compare the respective advantages and constraints of both methods. The FVM method involves discretising the fluid domain into a set of control volumes, and approximating the fluxes of mass, momentum, and energy across the boundaries of these volumes. This discretisation method is widely used in CFD simulations due to its ability to handle complex geometries and unstructured meshes while conserving mass, momentum, and energy, which are crucial for accurate simulations.

The 3D conservation equations (Eq. 1) for mass, momentum, and energy are solved together and coupled with the radiative transfer equation (RTE) in transparent (air) media using mostly the discrete ordinates (DO) model which performs a space discretisation in several solid angles (Nebbali et al., 2012) and makes it possible to cope with the integral term of the RTE. In greenhouse CFD studies, the global radiation distribution inside the canopy was initially assessed from the application of the Beer's law, for a vertical incident radiation or considering the sun's path in the sky (Nebbali et al., 2012). An extinction

coefficient within the canopy was also imposed. This simplified approach made it however difficult to correctly solve the energy balance inside the canopy.

But recently, thanks to an adequate parameterisation setting (Boulard et al., 2017) the radiative transfer equation (RTE) in semi-transparent (crop rows) media was solved along with the transfers in transparent (air) media using the discrete ordinates (DO) model. It means that the coupling between radiative and convective transfer was automatically performed by the CFD software for the solid and fluid interfaces and the canopy is considered as a semi-transparent medium interfering also with radiations. The net short waves radiative balance for each mesh of the crop cover is provided by the software and added to the net long wave radiative balance. This global net radiative flux is then considered as the source term of the energy balance equation that performs the computation of sensible and latent heat exchanges between each cell of the canopy and air.

2.2. Dynamic effect of the canopy on the airflow

2.2.1. Porous medium approach

As describing the geometry of the real plants inside the greenhouse remains quite complicated, requires a powerful computer, and is time-consuming, we consider plant rows as a porous medium in the shape of parallelepipeds consisting of a solid matrix (plants), crossed by a network of interconnected pores (air). It is also assumed that the solid matrix is rigid (or that it undergoes negligible deformations).

In the canopy, the size and distribution of the pores, simulated to the voids between the leaves and the branches, are irregular. Nevertheless, as noted above, providing a detailed description of the plants would be quite difficult, thus assimilating the canopy to a porous medium appears to be the best compromise to consider the influence of plants on the

283 airflow. Moreover, most CFD software consider the porous medium approach in a standard
284 way with respect to flow exchanges (Ansys-Fluent, 2010).

285 **2.2.2. Darcy-Forchheimer model**

286 While the traditional porous media model proposed by Darcy and completed by
287 Forchheimer (Kaviany, 1995) was initially developed to describe flows in porous media of
288 high density and low permeability, it can also be used to describe flow in crop rows, which
289 are high-permeability media (Bruse, 1995; Green, 1992).

290 Using Ansys Fluent Software facilities, crop rows are simplified and simulated to
291 parallelepipedal blocks of homogeneous porous medium (Figure 1).

292 The sink of momentum due to the drag effect of the crop is symbolised by the source
293 term S_ϕ in Eq. (1) and expressed by the unit volume of the cover by the commonly used
294 formula (Thom, 1971; Wilson, 1985):

295 $$S_\emptyset = -LADC_D v^2 \quad (2)$$

296 where v is the air speed within the crop cover, *LAD* is the leaf area density and C_D is a drag
297 coefficient. In addition, considering the crop as a porous medium, the pressure drop induced
298 by the drag effect can also be expressed through the Darcy-Forchheimer equation:

299 $$S_\emptyset = -\left(\left({}^{\mu}/_{K}\right)v + \left({}^{C_F}/_{K^{0.5}}\right)v^2\right) \quad (3)$$

300 where μ is the dynamic viscosity of the fluid, K the permeability of the porous medium and
301 C_F the non-linear momentum loss coefficient. For low air speed values observed inside the
302 canopy, the first term of Eq. (3) to the right can be neglected compared to the quadratic
303 one. Combining then Eqs. (2) and (3) yields:

304 $${}^{C_F}/_{K^{0.5}} = LADC_D \quad (4)$$

305

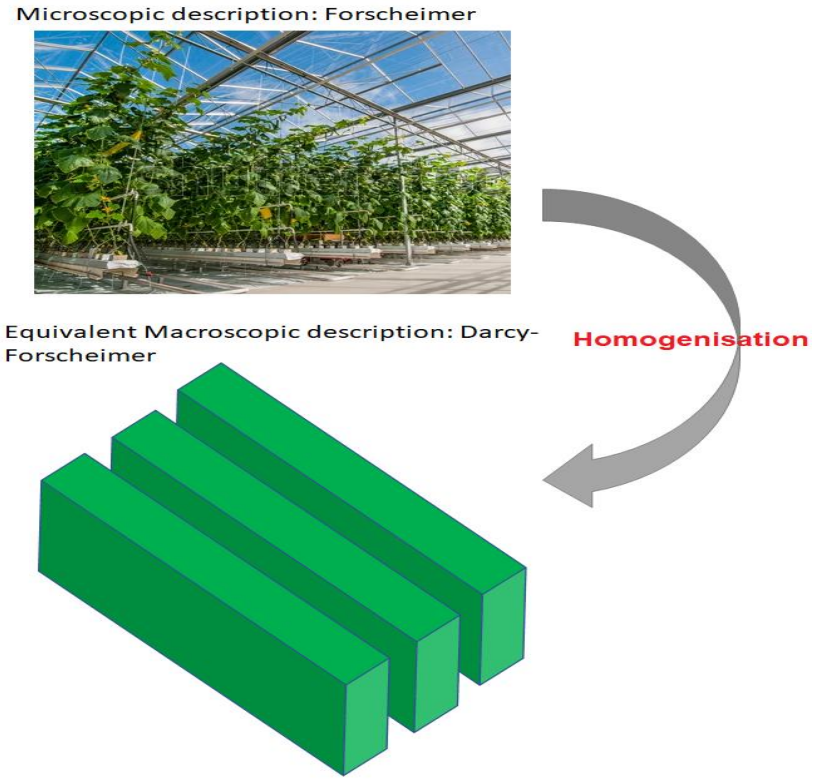

Fig.1 Description of the crop: homogenisation method

Consequently, as can be seen in Eq. (4) the only required parameters are the leaf area density (LAD) (i.e. leaf area divided by the canopy volume), which needs to be measured, and the discharge coefficient C_D which value depends on the considered plant distribution. A value of 0.30 for C_D was calculated by Green (1992) for a forest tree and of 0.20 was proposed by Bruse (1995) for plants associations in general. More recently, various greenhouse crops were installed in wind tunnel facilities to deduce their discharge coefficient. Thus, Haxaire (1999), Lee et al. (2006) and Sase et al. (2012), reported tomato crop drag coefficients of 0.32, 0.26 and 0. 31 respectively, while Molina-Aiz et al. (2006) found C_D values of 0.26, 0.23, 0.23, and 0.22 for tomato, bell pepper, eggplant, and bean, respectively, suggesting that the effect of leaf shape and size is not significant on the drag coefficient.

2.3. Sensible heat and water vapour exchanges between plants and air

2.3.1. Energy balance equation of crops

In addition to their influence on airflow, plants also significantly alter the overall energy and water vapour balances. Beyond considering the crop as a sink of momentum, it must also be considered as a volumetric source or sink of latent and sensible heat.

The constraints due to the complexity of crop geometry has led to adopt a macroscopic approach to describe the crop effects (Fig. 1). Thus, one can establish an energy balance equation for each elementary volume of the crop. According to this energy balance, the net radiation absorbed by the crop is equal to the latent and sensible heat exchanged (Fig. 2).

Due to the net radiation R_{abs} intercepted by plant leaves (mainly owing to solar radiation during the day), they exchange sensible (qs) and latent heat (ql) with the surrounding air. As Brown and Covey (1966) estimated that the heat stored in crops is less than 1%, the capacitive term of the energy equation is neglected, and the energy balance equation can therefore be expressed in a simplified way as:

$$R_{abs} + ql + qs = 0 \quad (5)$$

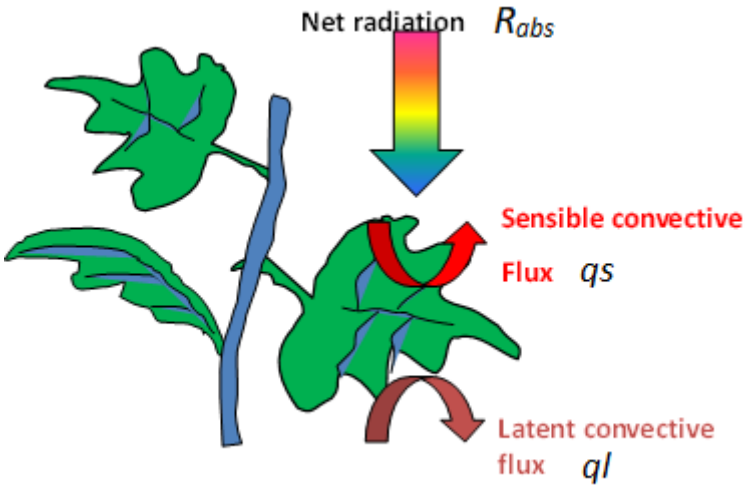

Fig. 2. Net radiation, sensible and latent heat balances of leaves

The crop stands (crop rows) in the greenhouse are represented by parallelepipeds arranged in n rows of length L, width l and average height H, characterised by their volumetric leaf area index LAD linking their leaf surface to their crop volume.

The energy balance equation of a volume element dV becomes:

$$R_{abs} - L_v\, E - 2\, LAD\, C = 0 \qquad (6)$$

where $R_{abs}$is the absorbed net radiation (W m^{-3}); $L_v\, E$ is the latent heat flux density (W m^{-3}), L_v being the heat of vaporisation of water (2440 10^3 J kg^{-1} at 20°C) and E, the evaporated water flux (kg m^{-3} s^{-1}); C is the sensible heat flux density (W m^{-3}). The absorbed radiation R_{abs} (W m^{-3}) in each cell of the canopy can be directly deduced from Beer's law, as described in Bouhoun Ali et al. (2017).

The sensible heat flux is evacuated by both sides of the leaf, hence the presence of a coefficient 2 in Eq (6) while the transpiration occurs mainly through the underside of the leaf (hypostomatic), however some plants transpire on both sides (amphistomatic leaves) like those of tomatoes (see Boulard et al., 1991) which upper side stomatal resistance is about 3 times higher than the lower one (equivalent to 3 times less stomatal apertures).

The sensible heat flux density C (W m^{-3}) corresponds to the convective exchanges between leaves and surrounding air and can be written as follows:

$$C = \rho C_p \frac{T_l - T_a}{r_a} \quad (7)$$

where C_p is the specific heat at constant pressure (J kg^{-1} K^{-1}); ρ is the air density (kg m^{-3}); T_l is the leaf temperature (K), T_a is the air temperature (K) and r_a the aerodynamic resistance (s m^{-1}).

2.3.2. Leaf transpiration

Ecophysiological transpiration models classically assume that the transfer of water vapor between the plant and the atmosphere follows a diffusion law proportional to the water vapor concentration gradient between leaf and ambient air. The total resistance between inside leaves and air is considered as the sum of two resistances in series (Fig. 3):

- the aerodynamic resistance r_a (s m^{-1}) between the ambient air and the leaf surface.

- the stomatal resistance r_s (s m^{-1}) between the sub-stomatal cavities and leaf surface.

Simulating transpiration with this approach thus requires determining leaf temperature in addition to the physical air and crop parameters.

To overcome this problem, another approach proposed by Penman (1948), and later modified by Monteith (1973), avoids considering leaf temperature to deduce transpiration according to more easily accessible physical quantities: the radiation absorbed by the canopy and the air vapour pressure deficit (Katsoulas and Stanghellini, 2019).

The latent heat density (transpiration rate density) is given by Eq. 8:

$$L_v E = \frac{R_{abs} + 2\rho \ LAD \ C_p \ VPD_a / r_a}{\Delta + 2\gamma \left(1 + \frac{r_s}{r_a}\right)} \quad (8)$$

where γ is the psychrometric constant (Pa K^{-1}), VPD_a is the air-air vapor pressure deficit (Pa), and Δ is the slope of the saturated water vapor pressure curve according to

temperature. Yet, as it is based on an approximation of the slope of the water vapour saturation curve, the leaf temperature has to be close to air temperature, which is not the case with dry and hot air.

All these approaches are based on the concept of the "big leaf", a large virtual leaf with the average properties of the canopy leaves, both from the climatic, stomatal, and aerodynamic conductance point of views. Although simplified, this virtual leaf concept has allowed the development of many transpiration models for a wide range of greenhouse crops: cucumber (Yang, 1995), rose and various horticultural crops (Baille et al., 1994 a, b), tomato, (Stanghellini, 1987; Boulard et al., 1991; Fatnassi et al., 2003, 2015; Bartzanas et al., 2004; Fidaros et al., 2010; Majdoubi et al., 2009, 2016; and Kim et al., 2021a, 2021b). Ornamental plant interactions with local environment in greenhouses were also studied by Fatnassi et al. (2006) for roses, by Kichah et al. (2012) and Bouhoun Ali et al. (2018) for New Guinea Impatiens and by Chen et al. (2015) for Begonia.

If one considers leaf temperature T_l, the water vapor flux between plants and air, E in kg m^{-2} K^{-1}, can be expressed as follows:

$$E = \rho LAD \frac{\omega_l - \omega_a}{r_t} \quad (9)$$

Where ω_l represents the absolute saturating humidity at leaf level and ω_a the absolute humidity of surrounding air in kg kg^{-1}, r_t is the total resistance (r_s+r_a) to water vapour (Lhomme and Katerji, 1991). ω_a is deduced from the solution of the species transport equation for the water vapour mass fraction. A recall of classical aerodynamic (r_a) and stomatal (r_s) resistance settings is provided in Appendix A.

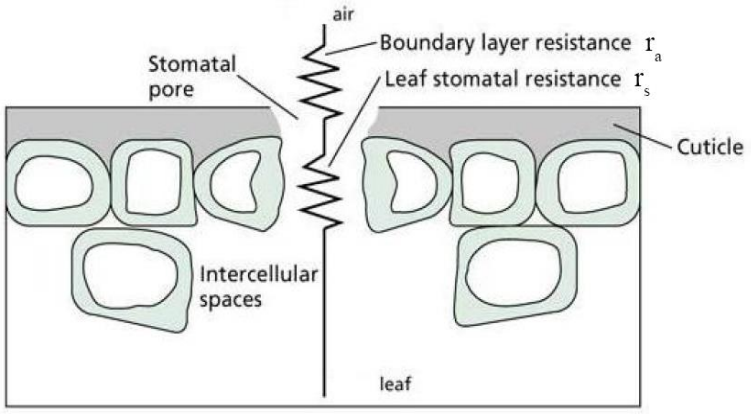

Fig. 3. Resistances to water vapor transfer between leaf and air.

2.4. Radiative transfers within the crop equivalent porous medium

The equivalent porous medium is a very flexible and versatile phenomenological approach that allows to consider not only the convective transfers but also the radiative ones. Thus, the canopy is considered as homogeneous and characterised by its extinction coefficient $K_{c,}$ and the incident global radiation follows a classical Beer-Lambert's law through the crop stands:

$$Rg(z) = Rg_0\, e^{-K_c LAD\, z} \tag{10}$$

where $Rg(z)$ is the global radiation along the optical path of the sun at a distance z from the top of the canopy, Rg_0 is the global radiation intercepted at the top of the crop cover, K_C is the radiation extinction coefficient which depends on the crop (Goudriaan, 1977; Guyot, 1999).

In the first greenhouse CFD studies, the solar distribution was inferred using simple models to determine the distribution of solar radiation within a greenhouse tunnel based on the path of the sun, greenhouse geometry, cover transmittance and sky conditions (Boulard and Wang 2002). Then most authors applied the Beer's law (Bartzanas et al., 2004; Fatnassi et al., 2006; Majdoubi et al., 2009) by providing the incident radiation at the top of the crop and an extinction coefficient within the crop cover to compute the vertical attenuation of

421 solar radiation inside the canopy. It is the reason why they have mainly considered
422 simulations when the sun was almost at zenith, i.e. around the solar noon and the summer
423 equinox. This approximation is valid when the crops are short, as it is the case for lettuces
424 (Boulard & Wang, 2002) or impatiens pot plants (Kichah et al., 2012). This simplified
425 approach made it however difficult to consider the directional nature of the solar radiation.
426 Thanks to an appropriate UDF accounting for the directional property of direct solar
427 insolation, Nebbali et al. (2012) were the first to consider global radiation penetration inside
428 the canopy on a very realistic way for a tomato crop in a tunnel greenhouse (Fig. 8). They
429 numerically deduced the solar radiation distribution inside tomato stands but they did not
430 undertake experimental validation of their model extinction coefficient within the crop
431 cover and assuming a vertical transfer. Unfortunately, their UDF lacks genericity and could
432 hardly be reusable for other greenhouses and crop types.

433 More realistic results were obtained by simultaneously solving the radiative transfer
434 equation (RTE) and convective heat transfer equation. The main difficulty, however, arose
435 from the nature of the radiative transfers that involve surface-to-surface interactions and
436 may differ from one wavelength to another for a given medium. The discrete ordinate (DO)
437 method is often used since it offers a good compromise between accuracy, computational
438 economy and flexibility. Moreover, it was adapted in commercially available codes such
439 as Ansys Fluent to take account of the variation of the optical properties of the cover
440 according to the wavelength range. The main difficulty is that accounting for radiative
441 transfers requires specific developments. In recent studies, the spectral intensity radiation
442 within the air was determined by solving the radiative transfer equation (RTE) using the
443 DO radiation model (Ansys-Fluent, 2010) divided into 2 bands where the radiative and
444 optical parameters are considered as constants: from 0.4 to 2.4 μm for solar radiation and

445 from 2.4 to 180 μm for terrestrial long wave radiation (Bournet et al., 2007; Nebbali et al.,
446 2012).

447 The model was then improved by solving the radiative transfer equations using the
448 same model (DO) within the whole studied domain including the crop cover (Boulard et
449 al., 2017). In this prospect, the canopy was considered, as a semi-transparent medium with
450 optical properties adequately expressed in terms of coefficients of extinction and refractive
451 indexes compatible with the use of the DO radiative application (see Appendix C of
452 Boulard et al., 2017). Considerable efforts still need however to be done to include the
453 interchange of short and long wavelength radiation between the sky and the greenhouse
454 cladding, and between greenhouse structural elements (roof, screens, structural elements,
455 shelves, canopy…).

456 **2.5. Condensation on leaves**

457 As condensation of liquid water on greenhouse crop leaves is responsible for the
458 development of major fungal diseases like grey mould (Botrytis C.) which strongly devalue
459 the yields (Nicot & Baille, 1996), the study of this mechanism has recently stimulated
460 several simulation studies based on a CFD modelling approach, particularly for
461 Mediterranean and Chinese solar greenhouses (CSG) where this question is recurrent.
462 Basically, it also requires a module of condensation, based on similar aerodynamic
463 resistance of leaves than previously presented. Condensation risks generally first occur
464 along roofs and walls that may become colder than inside air or leaves due to radiative
465 losses at night. Condensation involves a water uptake from the ambient air along the wall
466 and roof surface, and then on the leaves (which are generally colder than the ambient air),
467 which occurs when the local temperature goes below the dew point. In CFD model, it is
468 expressed as a mass flux sink term in the water vapour transfer equation. A thorough

description of the condensation model may be found in Bouhoun Ali et al. (2014). The total rate of mass condensation flux is calculated from Bird et al. (1960) and the corresponding UDF was adapted from Bell (2003). Piscia et al. (2012) studied the response of a CFD model to a step-change in night-time transpiration from the crop. The previously mentioned studies mainly focused on condensation risks on walls and roofs, and it is only recently that Liu et al. (2021) developed a CFD model to study the spatial and temporal distribution of the indoor microclimate and condensation on cucumber leaves in a CSG at night. An et al. (2022) also considered a CSG but for tomato plants and carried out a similar approach for both diurnal and nocturnal conditions.

2.6. CO_2 exchange between plants and air

Due to photosynthesis and respiration, CO_2 is exchanged by leaves with atmosphere through stomata in the same way as for the water vapour exchange. So, these processes have been modelled by considering the absorption or production of CO_2 of plants as sink or source term S_ϕ in Eq. (1) where the state variable is the $[CO_2]$ instead of $[H_2O]$.

Roy et al. (2014) have used a UDF to include a photosynthesis model of the absorption or production of CO_2 (Thornley, 1976) produced by the plants in a semi-closed greenhouse with a tomato crop and CO_2 supply. For their simulations, they considered a 3D model of a cropped greenhouse, including a discrete CO_2 injection system and an air-cooling and dehumidifying system. Comparisons between the simulated and the measured values of the CO_2 concentration inside the greenhouse were done for a whole day time. CFD simulations correctly predicted the time course for the net CO_2 consumption per greenhouse surface unit. Up to now however, to our knowledge, no other work has been published on that topic although it is of high interest and probably deserves more attention in the coming years.

493 Several expressions of the photosynthesis process are available as source term,
494 Manzoni et al. (2011) expressed it for an elementary crop volume as a multiplicative
495 function of light and CO_2 limitation terms, the CO_2 limitation term being obtained by
496 linearising the Rubisco limited photosynthesis kinetics; Reichrath et al. (2001) and Molina
497 et al. (2017) use the Acock's model which already integrates vertically photosynthesis
498 along the entire crop stand profile. Roy et al. (2014) and Boulard et al. (2017) followed the
499 model of Thornley (1976) to simulate the absorption or production of CO_2 produced by the
500 plants in a semi-closed greenhouse with a tomato crop and CO_2 supply. For their
501 simulations, they considered a 3D model of a cropped greenhouse, including a discrete CO_2
502 injection system and an air-cooling and dehumidifying system. They calculated the raw
503 photosynthesis flux P_r for an elementary crop volume, which is more in line with the
504 phenomenological approach that considers reduced volumetric elements:

505 $$P_r = \frac{\alpha I \tau \rho C_a}{\alpha I + \tau \rho C_a} LAD \quad (11)$$

506 where α is the photosynthesis efficiency (α=1.01 10^{-10} kg CO_2 J^{-1}); I (W m^{-2}) is the PAR
507 incident radiative flux, τ is the leaf conductance ($1/(r_a+r_s)$), and C_a is the concentration of
508 CO_2 in surrounding air. It is worth noticing that with respect to water vapour transfers, the
509 resistances to CO_2 transfer must be corrected, based on the difference of diffusivity in air
510 between CO_2 and H_2O (Manzoni et al., 2011) with: $r_{sc}=1.65r_{sw}$ and $r_{ac}= 1.34r_{aw}$; the
511 subscripts *c* and *w* refer to CO_2 and H_2O respectively.
512 The production of CO_2 consists in the maintenance and growth respirations which together
513 can be estimated for tomato crop to 22% of the raw photosynthesis consumption (see
514 complementary details in Boulard et al. (2017)), hence the net photosynthesis consumption
515 flux S_{CO2} is:

516 $$S_{CO2} = 0.78P_r \quad (12)$$

3. Numerical implementation

3.1. UDF description

Thanks to the possibility to customise CFD software, heat and mass exchanges between the plant and the greenhouse air are introduced in the CFD model through the addition in equation 1 of source/sinks terms describing these transfers. Following Boulard &Wang (2002), each mesh of the crop cover is simulated to a "volume heat source" of porous medium absorbing a radiative flux, R_{abs} (Eq. 10). This flux is partitioned into convective sensible (q_s) and latent (q_l) heat fluxes (water vapour) according to Eq. (5), which themselves depend on the aerodynamic (r_a) and stomatal (r_s) and resistances between the virtual solid matrix representing the crop and the local climate characterised by air (T_a) and leaf (T_l) temperatures and absolute humidity (ω_a).

The expression of the latent heat flux requires the calculation of the water vapour concentration ω_l which can be obtained from the leaf temperature T_l according to the Magnus Tetens law for the saturated water vapour pressure:

$$\omega *_{T_l Tl} = 610.5\, e^{(17.269 T_l / 237.3 + T_l)} \quad (13)$$

As r_a and r_s depend on the local climate (but also on the plant substrate water status (see Appendix A), a close coupling between the crop and air flow is thus operated. Finally, we get a system of two equations with two unknowns which are additional outputs of great interest, determined into each mesh of the crop cover: the leaf temperature (T_l) and (ω_l) the latter allowing to deduce the value of the latent heat flux associated with the transpiration of the cover *E* following Eq. (9).

CFD software makes it possible to specify the above mentioned latent and sensible heat fluxes as source terms for the conservation equation (Ansys-Fluent (2010)). Source

type boundary conditions are then applied to each crop row to simulate plant activity. To describe the source term $S_{\emptyset}$ of the conservation equation, CFD software such as Fluent Ansys™ uses most of the time a relationship of the form:

$$S_{\emptyset} = A + B.\emptyset \quad (14)$$

where A and B must be identified regarding to the volumetric latent and sensible heat expressions provided by Eqs (7) and (8).

For the temperature:

$$A = \frac{2*LAD\rho C_P}{r_a} T_l \text{ and } B = -\frac{2*LAD\rho C_P}{r_a} \quad (15)$$

For the water vapor content:

$$A = \frac{LvLAD\rho C_P}{(r_a+r_s)} \omega_l \text{ and } B = -\frac{LvLAD\rho C_P}{(r_a+r_s)} \quad (16)$$

The equations describing r_s (see Appendix A) are also solved by means of a UDF specially developed for this purpose and coupled with the main CFD solver which provides the local climate parameters within each mesh (Figure 4). The connection between the crop submodel routine and the main solver is described in Fig. 4.

The output of the crop submodel is the leaf temperature which is deduced from the energy balance over the crop by combining Eqs (6), (7) and (8):

$$T_l = \frac{r_a}{2LAD\rho C_p} (R_{abs} - \text{ql}) - T_a \quad (17)$$

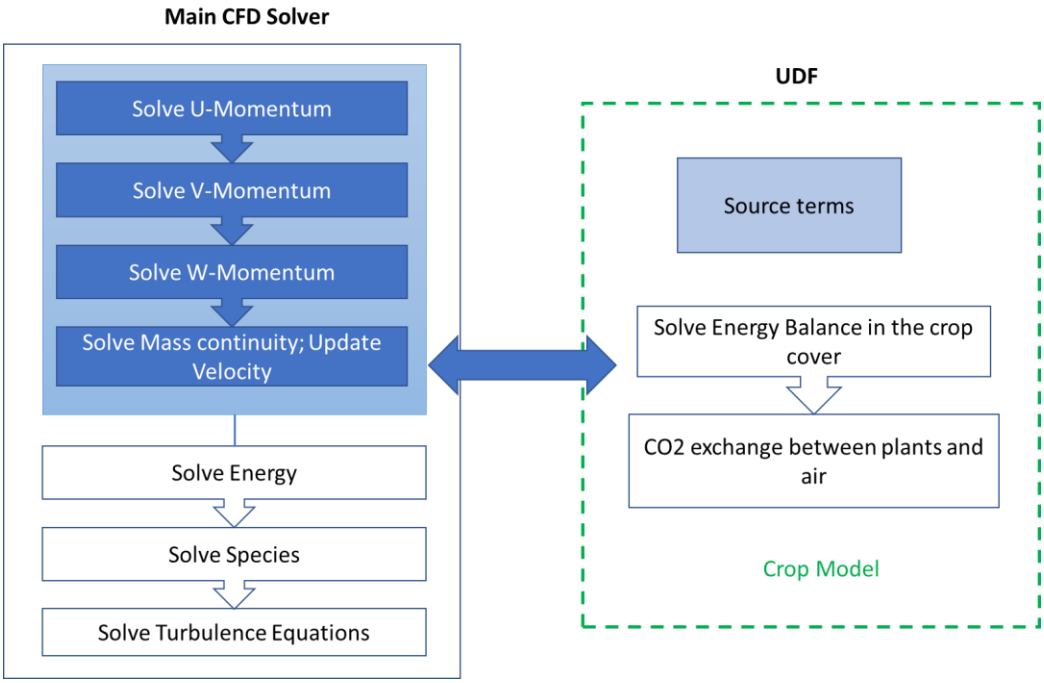

Fig. 4 Sketch of the exchanges between the UDF and the main solver in the CFD model.

3.2. Mesh and boundary conditions

Following Boulard & Wang (2002), the calculation domain includes most of the time the greenhouse and its close environment (Fatnassi et al., 2003, 2006; Majdoubi et al., 2009, 2016; Nebbali et al., 2012), but it can sometimes be restricted to the inside volume of the greenhouse if the boundary flow conditions at the greenhouse surface are known (Kichah et al., 2012; Boulard et al., 2017; An et al., 2022). Inside the greenhouse, the crop stand is considered as a porous medium, with the same geometry and dimensions as in reality.

If the calculation domain includes the greenhouse and its close environment, an inlet logarithmic velocity profile or power law profile corresponding to the measured wind profile is generally imposed at the entrance of the calculation domain, along with the air temperature, and water mass fraction values (and [CO_2] concentration if necessary). The radiative flux is also imposed at the upper limit of the calculation domain. At the outlet of the calculation domain, all variable gradients are generally set to zero, except for the

pressure. The temperature of the walls, roof, and soil surfaces are deduced from an energy balance over these surfaces.

The computational grid is refined near solid boundaries i.e. soil, walls, and roof where stronger gradients of the variables of interest (velocity, temperature…) are expected. Tests of independency of the grid regarding the results are generally undertaken to optimise the cell numbers and distribution with the aim to limit the required CPU time to get a reliable solution.

3.3. Validation of CFD model

The validation of the CFD model is generally conducted through the comparisons of computed and measured greenhouse climate fields (air temperature and humidity but also sometimes CO_2 concentration, wall and ground temperatures, leaf temperature) or flux measurements (air speed, crop transpiration, condensation fluxes, radiation) as well as global air exchange rates (Table 1). The first validations were performed using state variables such as air speed, air, and leaf temperatures (Haxaire, 1999) for tomato crop and transpiration fluxes (Boulard & Wang, 2002) for lettuce crop. Later, Fatnassi et al. (2002, 2003, 2015) and An et al. (2022) have used networks of sensors to monitor temperature and humidity in horizontal and vertical plans inside the greenhouse. Recently, Boulard et al. (2017) mapped CO_2 and Liu et al. (2021) water condensation on the plastic roof and cucumber leaves with similar 3D validation approach. Thanks to the existence of stable wind regimes like *Mistral* in the lower Rhone valley or coastal winds on the Moroccan Atlantic shore, one can also displace the sensors all along the greenhouse volume to map air temperature or humidity while normalising the measured values with respect to outside wind, which is the main driving force of greenhouse ventilation (Haxaire, 1999; Majdoubi et al., 2009). All these measurements have been confronted to simulated data and they

599 generally confirm the accuracy of the model to produce the microclimatic flow fields inside
600 the greenhouse, including the crop stands.
601
602 **Table 1.** Validation studies of the CFD model based on the comparison between measured
603 and simulated values of climate parameters in the greenhouse

Authors	Greenhouse type	Crop	Dimension	Validation
Boulard & Wang (2002)	Tunnel	Lettuce	3D steady	Transmittance, air velocity Temperature, transpiration flux
Fatnassi et al. (2003)	Moroccan type	Tomato	3D steady	Ventilation rate
Bartzanas et al. (2004)	Tunnel	Tomato	2D/3D steady	Air velocity, ventilation rate, air temperature
Fatnassi et al. (2006)	Multi span	Roses	3D steady	Ventilation rate
Majdoubi et al. (2009)	Canary type	Tomato	3D steady	Air temperature, relative humidity
Tong et al. (2009)	Chinese	Lettuce	2D unsteady	Air temperature
Boulard et al. (2010)	Multispan plastic	Roses	2D unsteady	Air temperature and humidity, spore concentration
Piscia et al. (2012a)	4-span plastic	Lettuce	3D unsteady	Air temperature, roof temperature, humidity ratio
Tamimi et al. (2013)	Arch type	Tomato	3D steady	Air velocity, evapotranspiration, stomatal resistance
Majdoubi et al. (2016)	Canarian	Tomato	3D steady	Air temperature and humidity
Bouhoun Ali et al. (2018)	Venlo glass house	New Guinea Impatiens	2D unsteady	Air temperature, leaf temperature matric potential, stomatal resistance, air humidity, transpiration rate
Boulard et al. (2017)	6-span glasshouse	Tomato	3D unsteady	Air temperature, leaf temperature, saturated humidity at leaf temperature, air humidity, shortwave radiation, air speed, crop transpiration, CO_2 concentration
Bouhoun Ali et al. (2019)	Venlo glass house	New Guinea Impatiens	2D unsteady	Air temperature and humidity, stomatal resistance, ventilation rate
Fatnassi et al. (2021)	Four-span plastic arched greenhouse	Rose	3D unsteady	Air temperature and humidity

604

605 # 4. Main results from CFD studies including a crop submodel

606 Following the pioneer works of Haxaire (1999) and Boulard and Wang (2002),
607 Bartzanas et al. (2004), Fatnassi et al. (2003, 2015), Fidaros et al. (2010), Majdoubi et al.
608 (2009, 2016), An et al. (2021) developed CFD simulations with crop sub-models,
609 principally for tomatoes but also for cucumber (Liu et al., 2022). Ornamental plant
610 interactions with local environment in greenhouses was also studied by Fatnassi et al.
611 (2006, 2016) for roses, Kichah et al. (2012) and Bouhoun Ali et al. (2018, 2019) for New
612 Guinea Impatiens and by Chen et al. (2015) for Begonia.

613 **4.1. Milestones of CFD crop model developments**

614 Figure 5 depicts the milestones of crop model developments. Since the pioneering
615 works of Boulard & Wang (2002) who included both the momentum sink terms and the
616 sensible/latent source terms in the conservation equations for water mass fraction,
617 momentum, and energy, several improvements of the model have been undertaken. This
618 model was recently adapted to consider the simulations of the crop behaviour under
619 suboptimal water inputs that may lead to stomatal partial closing and transpiration rate
620 reductions, as is often the case in real situations (Bouhoun Ali et al. 2018, 2019).

621 Radiative transfer within the crop itself is still a major concern since it determines the
622 two main physiological crop functions: transpiration and photosynthesis. The
623 determination of the global radiation in each cell is therefore required. It was first assessed
624 from the application of the Beer's law (Fanassi et al. 2003; Bartzanas et al. 2004, Fatnassi
625 et al., 2006, Majdoubi et al., 2009) knowing the incident global radiation at the top of the
626 canopy, before improvements were made by solving the Radiative Transfer Equation (RTE)
627 first in the domain surrounding the crop, and then inside the crop itself (Fidaros et al., 2010;
628 Nebbali et al., 2012; Morille et al., 2013; Bouhoun Ali et al., 2018, 2019).

629 CO_2 exchanges and photosynthesis were included in CFD models by Roy et al. (2014)
630 and Boulard et al. (2017) who have considered the absorption or production of CO_2 by the
631 plants in their models.

632 In parallel, a special attention was paid to include condensation process in the
633 simulation through a specific subroutine determining the water uptake from the air and
634 corresponding heat flux along the walls and roofs (Tong et al., 2009; Piscia et al., 2012a,
635 b; Bouhoun Ali et al., 2014), but it is only very recently that condensation potentially
636 occurring along the leaves was introduced in the CFD approach (Liu et al., 2021, An et al.,
637 2022).

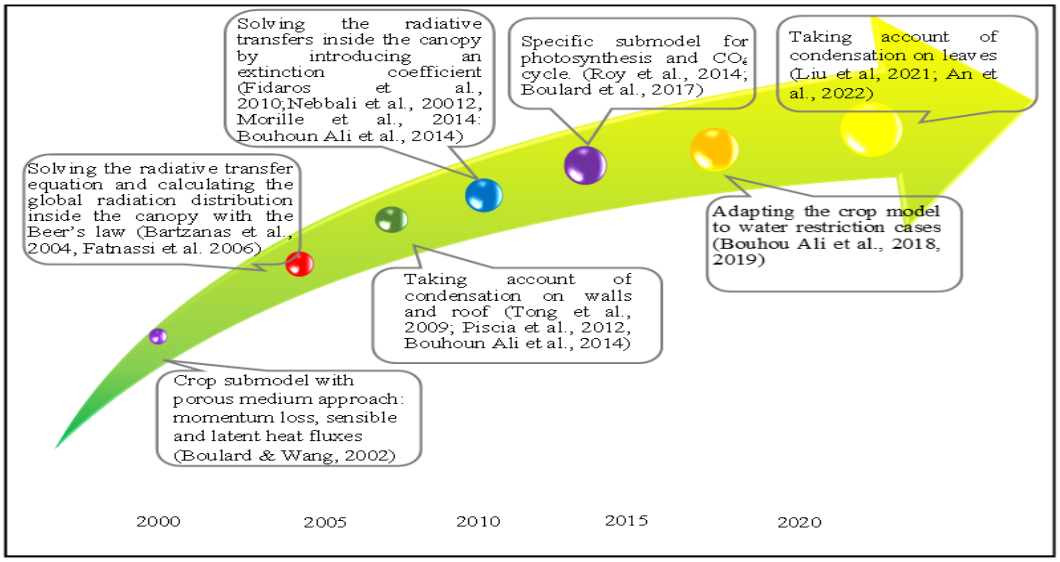

638

639 **Fig. 5** Milestones of CFD crop submodel developments

640 **4.2. Distribution of leaf temperature, crop transpiration and shortwave radiation**
641 **inside the crop**

642 Following the progress in CFD modelling, simulations gained in accuracy and made
643 it possible to assess interactions of the crop with the local environment into details.
644 Pouillard et al. (2012) have considered an experimental closed greenhouse with a tomato
645 crop to assess the radiation distribution inside the greenhouse including the crop stands.

They solved the radiative transfer equation, using the Discrete Ordinate model with a proper parameter setting concerning the optical properties of the semi-transparent medium simulated to the porous medium and distinguishing short from long wave radiations. Implementing a crop submodel encapsulated in a UDF dynamically linked with the main solver, they simulated the distribution of leaf temperature, air temperature and crop transpiration within the crop based on air velocity and surrounding climate parameters (Fig. 6).

Their results evidenced that the heterogeneity of the climate inside the greenhouse affects plant activity as illustrated in Fig. 6 showing the distributions of leaf temperature, crop transpiration and short waves radiations received within a tomato plant stand. They also showed that for this greenhouse, at the upper part of the crop stand, 2/3 of the captured radiative energy was transferred to latent heat thus increasing air humidity while only the remaining part contributed to greenhouse air warm up and heat accumulation higher. They also predicted that in the middle and lower parts of the crop, the latent heat associated with transpiration was higher than the received radiative energy, meaning that the leaves cooled the air at these levels.

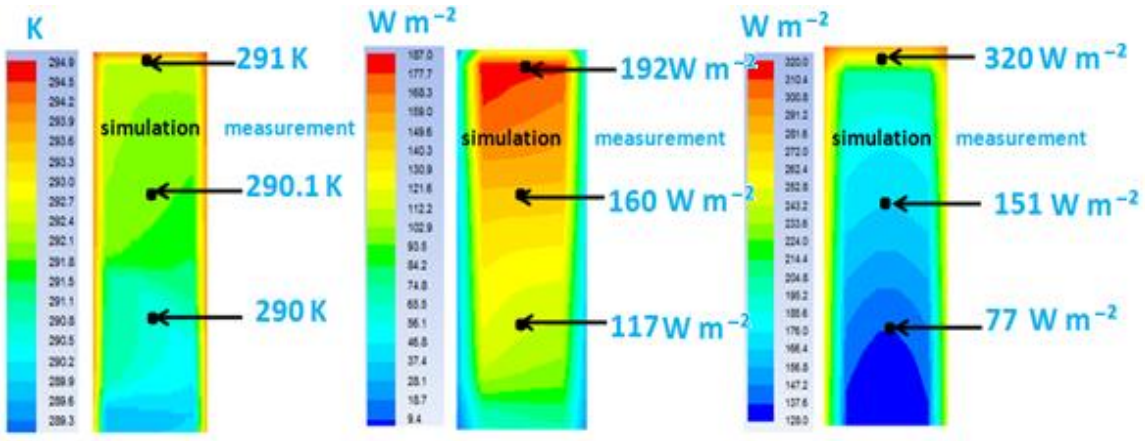

Fig. 6 Simulated and measured distributions of leaf temperature in K (left), latent heat of crop transpiration in W m^{-2} (middle) and short waves radiations in W m^{-2} (right) within the crop cover at noon (after Pouillard et al., 2012).

Using the same approach and implementing a module of solar transmission inside the crop cover, Nebbali et al. (2012) got very realistic results (Fig. 7), making it possible to assess the heterogeneity of crop transpiration and its evolution with the sun path all day long. Nevertheless, they did not undertake any validation of their model against experimental data.

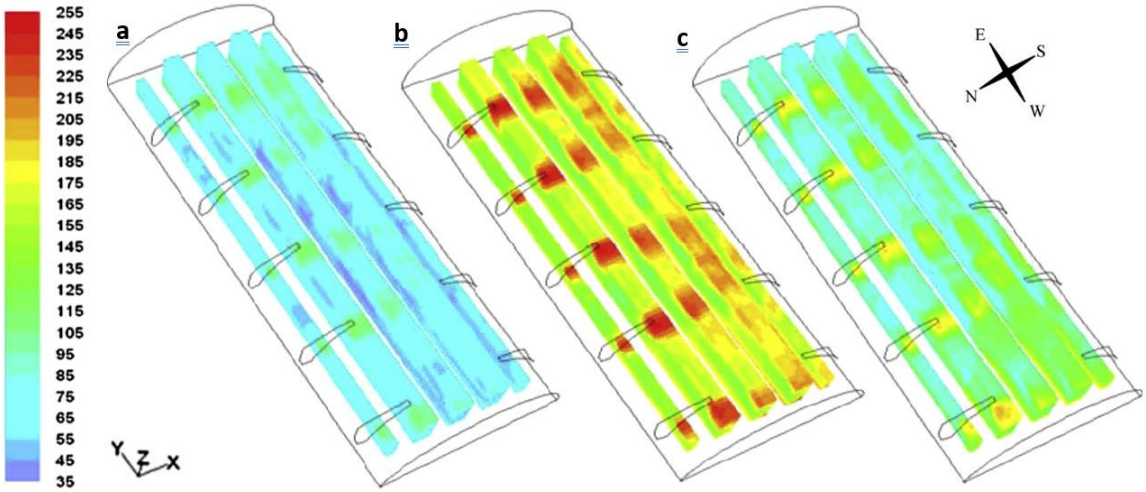

Fig. 7 Distribution of the transpiration heat flux density on June 21st. (a): at sunrise, (b): at midday, (c): at sunset (after Nebbali et al., 2012).

Bournet et al. (2017) carried out two-dimensional unsteady simulations at a daily timescale including crop interaction and sun path. The radiative transfer equation (RTE) was solved, based on the Discrete Ordinates method distinguishing short and long wavelength radiations. The ground was also meshed to simulate conduction. The model was run for a typical sunny day under temperate climatic conditions and validation was undertaken based on seven different parameters including temperature and relative

humidity of the air above and inside the crop, ground temperature, leaf temperature and transpiration rate (Fig. 8). Simulations stress the ability of the model to correctly predict the response of the greenhouse to a variation of the outside climate. In particular, the strong influence of the solar radiation was demonstrated. Although leaf temperature and transpiration rate were satisfactorily simulated, as well as local air humidity and temperature just above the canopy. The air temperature inside the canopy was however a little bit overestimated, and humidity underestimated suggesting that the air movement inside the canopy could be overestimated maybe because of an underestimation of the drag force of the porous medium.

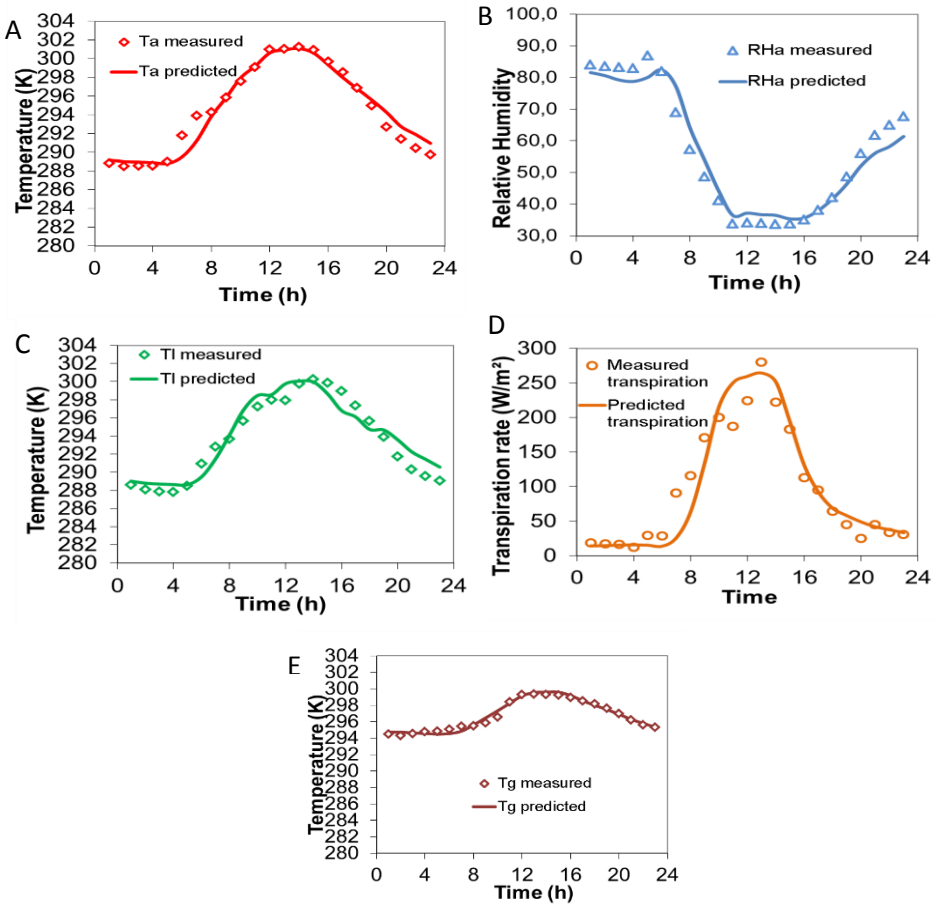

Fig.8 Comparison of measurements and CFD simulations for A) air temperature above the crop; B) relative humidity above the crop; C) leaf temperature, D) transpiration rate and E) soil surface temperature (adapted from Bournet et al., 2017).

Bouhoun Ali et al. (2018) adapted the crop model for cases when plants are subject to water restriction. In this prospect, they calibrated a multiplicative stomatal resistance expression depending not only on the meteorological parameters, but also on the soil water potential (Cannavo et al., 2016) and developed a submodel to calculate the water balance over the substrate. This model demonstrated its ability to predict the decrease of water availability in the substrate and that both stomatal resistance, air and leaf temperatures inside the canopy were higher for the water restricted conditions than for the well-watered one. It also showed that transpiration rates were lower for plants under water restriction (Figure 9), due to stomatal partial closing and transpiration rate reduction.

The same model was then implemented by Bouhoun Ali et al. (2019) for six different irrigation regimes, reducing progressively the water inputs. From the simulations, the scenario with 70% water supply (considering well water plants as the reference) appeared as a good compromise between the maintenance of plant activity and water saving, together with a reduction of fungal diseases or mould development risks. CFD simulations could, hence, improve water management strategy and identify microclimate conditions adapted to plant growth while reducing water inputs. It must be stated however, that the authors did not investigate the impacts of water restriction on plant architecture and quality which condition the marketing criteria.

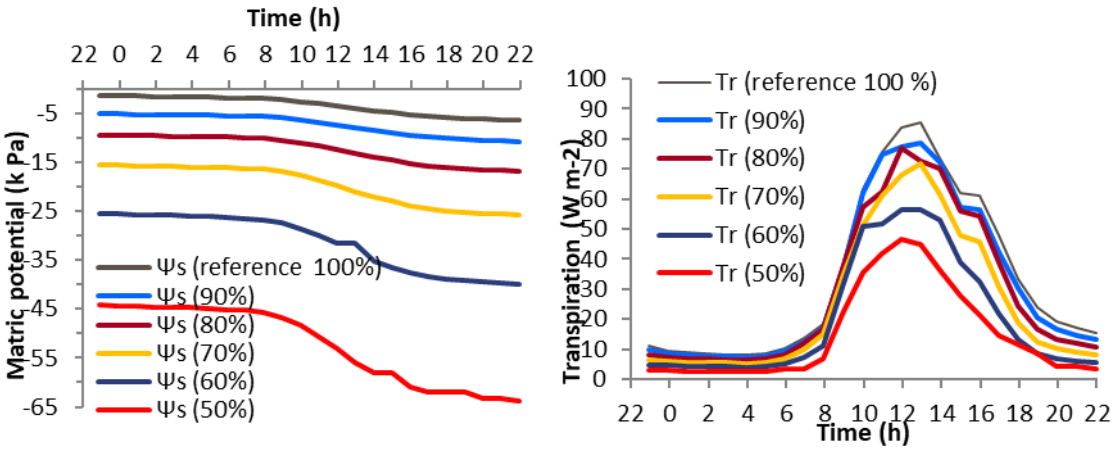

Fig. 9. Evolution of the matric potential in the ground (a) and corresponding evolution of the evapotranspiration predicted by a CFD model for an impatiens crop (b) (after Bouhoun Ali et al., 2018)

4.3. Simulation of the distribution of CO_2 concentration in the greenhouse

CFD makes it possible also to investigate the carbon dioxide fluxes associated with the photosynthesis and respiration processes. This has allowed mapping the CO_2 and H_2O concentrations in air, together with temperature inside cropped greenhouses often equipped with CO_2 injection systems. Reichrath et al. (2001) were to our knowledge the first to be interested in including the crop total carbon dioxide uptake rate for photosynthesis in CFD modelling. Following Acock's suggestion they divided the crop into three layers and showed that the top layer consumes 66% of total carbon dioxide, the middle one 27%, and the bottom one only 7%. In their simulations, the carbon dioxide injection and absorption by the crop were added to a two-dimensional CFD model and applied to a 60-span Venlo type glasshouse. Carbon dioxide dispersion was simulated, and revealed a higher concentration at the leeward part of the glasshouse due to less efficient ventilation compared to the windward side of the greenhouse (Fig. 10).

Fig.10 Carbon dioxide dispersion in a 60 span Venlo-type glasshouse with crops (after Reichrath et al., 2001).

More recently, Roy et al. (2014) and Boulard et al. (2017), investigated the 3-dimensional distribution of CO_2 in a closed plastic-greenhouse using both numerical, including a CFD crop model, and experimental approaches. In their study, the CO_2 concentration was solved by adding a transport equation for the CO_2 mass fraction in the 3-D CFD model, and using the porous medium approach coupled with crop eco-physiological and radiative transfer models. Transpiration and photosynthesis fluxes were considered as a function of this concentration and other microclimatic parameters.

They could predict the distribution of CO_2 concentrations in the greenhouse at various times of the day (Fig. 11, a-d). For example, at 8:00 am the greenhouse was closed, and CO_2 was supplied, which corresponds to higher concentration zones appearing near ground and injection pipes (Fig. 11a). As the greenhouse was always maintained closed at 11h 30 (Fig. 11b) CO_2 concentration was still very high at the bottom of crop rows (1200 ppm) near the injection pipes. Due to ventilation needs, injection was turned off at 1h pm (Fig. 11c) leading to a severe depletion (300 ppm) at crop level, due to an intense uptake for

765 photosynthesis. At 5:30 pm the greenhouse was again closed, and the CO_2 injection was
766 turned on again (Fig. 11d), leading again to higher concentration zones near the injection
767 pipes and a strong stratification.

768

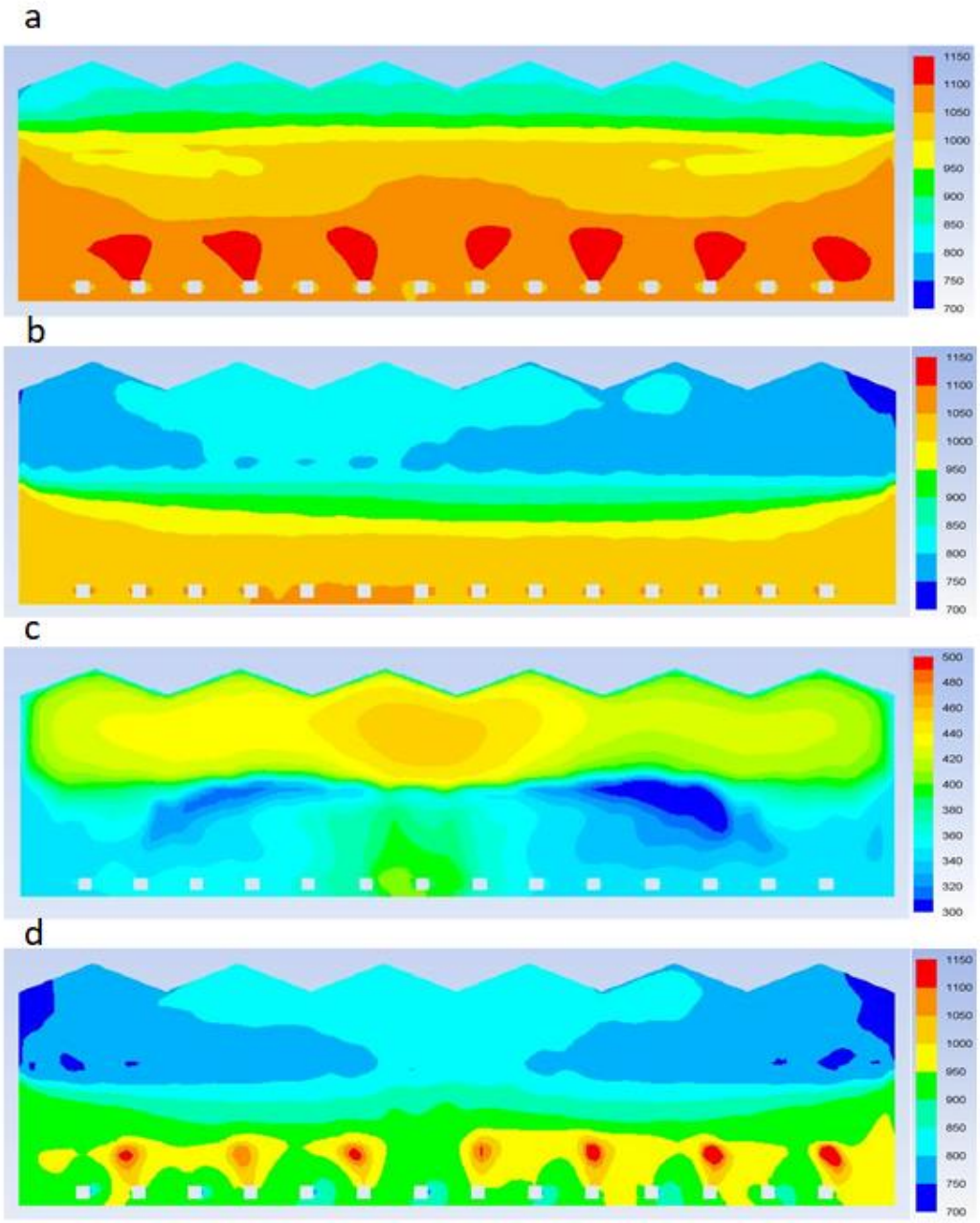

769

Fig. 11. Simulated carbon dioxide levels (ppm) in a median vertical transverse plane of the greenhouse at (a) 8:00 am; (b) 11:30 am; (c) 1:00 pm; (d) 5:30 pm. (After Boulard et al., 2017).

Molina-Aiz et al. (2017) implemented a CFD model to simulate photosynthesis in an Almeria-type greenhouse without CO_2 injection by incorporating the Acock's model by means of UDF's and the modelled CO_2 distribution shows a depletion in the leeward part of the greenhouse, where are situated the plants which absorb CO_2 (Fig. 12). The concentration of CO_2 in the windward part of the greenhouse was like the outside value, indicating that natural ventilation was sufficient to maintain an adequate concentration for the plants.

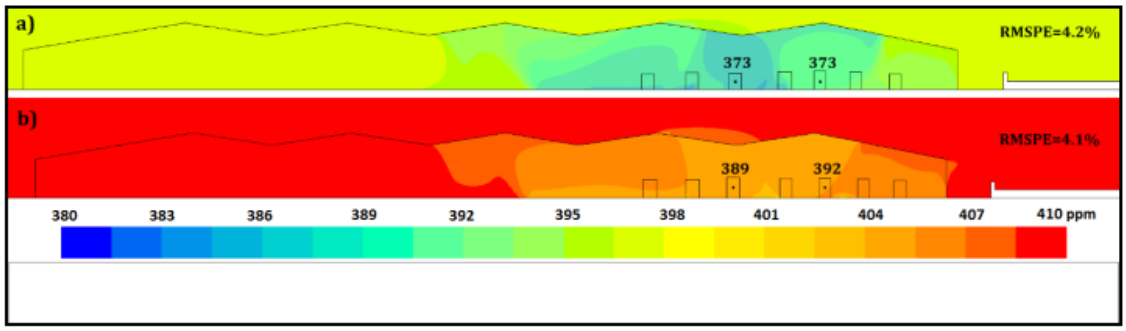

Fig. 12. Distributions of CO_2 concentration simulated with CFD and measured values (indicated in the figures) in the greenhouse on (a) 3/11/2014 and (b) 3/13/2014. (After Molina et al., 2017)

4.4. Simulation of condensation

Condensation is a key phenomenon in greenhouse management, not only because it may partly compensate water inputs due to evapotranspiration, thus reducing the water content of the air and consequently the absolute humidity, but also because condensation enhances risks of fungal developments or other diseases. To our knowledge, Tong et al. (2009) were probably among the first to take account of condensation in their CFD approach applied to

791 a closed, empty Chinese Solar Greenhouse. Their numerical model included specific source
792 terms derived from the formula suggested by Garzoli (1985) for the condensation that
793 occurred along the walls when the local temperature goes below the dew point. The latent
794 heat was then applied as an equivalent heat source to the roof where condensation occurred.
795 A more formalised model based on local steady state balance for the sensible heat and water
796 vapor was applied by Piscia et al. (2012) to a closed greenhouse. They conducted a
797 comprehensive analysis of the condensation process during night-time conditions and
798 determined the water uptake from the air by adapting a specific subroutine developed by
799 Bell (2003) based on the equation provided by Bird et al. (1960). In their study, however,
800 Piscia et al. (2012) considered the crop as a constant source of water vapor, thus neglecting
801 the interaction of the crop with the ambient climatic conditions. Moreover, they determined
802 the water uptake from the air, but omitted the associated heat flux along the walls. Bouhoun
803 Ali et al. (2014) conducted a CFD study for an Impatiens New Guinea greenhouse crop in
804 which water uptake from the ambient air along the roof surface, was expressed as a mass
805 flux sink term in the water vapor transfer equation. The corresponding source term for the
806 energy equation could then be obtained by multiplying the mass flux by the latent heat of
807 vaporisation. In particular, their results revealed the ability of the model to predict both the
808 air and wall temperatures of the greenhouse. In their recent paper, Liu et al. (2021)
809 simulated both the distributions of roof condensation and leaf condensation (Fig. 13). The
810 condensation on the leaves at 9 measurement points was observed manually for comparison
811 with the simulation results each hour from 18:30 to 5:30. They observed that condensation
812 always occurred earlier than the simulated condensation. They also reported that
813 condensation always appeared first on the roof rather than on the leaves. Focusing on the
814 Leaf Wet Duration (LWD) as an indicator of risk of fugal development, they predicted an

average error between the observed and simulated LWD of 1.25 h for the two studied days. They concluded that the crop canopy condensation model is appropriate to quantify the dynamics of water vapour and energy, even though, the model is expected to improve performance in a variety of scenarios.

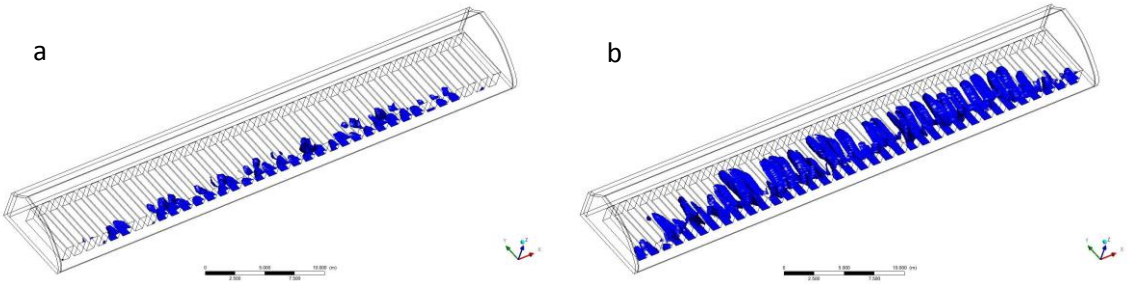

Fig. 13. Simulated leaf condensation on April 17 at (a) 01:30 and (b) 05:30. Y represents the north; X represents the east; and ■ represents the condensation that appeared based on simulation (after Liu et al., 2021).

5. Future trends

Despite the stated advances in CFD based plant activity modelling in greenhouses, further improvements still have to be conducted to reach a higher degree of realism.

5.1. A better consideration of radiation transfer in the crop stands

Given the complexity of radiative transfer into the whole greenhouse, with various light qualities (short and long waves; diffuse and direct light) interacting with different media (solid, diopters, transparent, diffuse), numerical simulations must consider the entire range of these exchanges, particularly between the leaves and other surrounding surfaces. Still, considerable efforts need to be done to include the interchange of short and long wavelength radiation between the sky and the greenhouse cladding, and between greenhouse structural elements (roof, screens, structural elements, shelves, canopy…). Indeed, for most of the

existing studies, the radiative transfers were considered less important than the convective ones and consequently largely simplified, even if the increase in the performance of the computer facilities and model developments made it possible to considerably improve radiation considerations in CFD modelling tools and offers new perspectives.

In addition, model microclimate validations with respect to light measurements are very rare, whereas greenhouse plant production directly depends, through photosynthesis and transpiration, on this parameter. Accordingly, a double effort must be performed (i) on the adaptation of the available radiation models of the CFD packages to the various radiative transfers, including inside the equivalent porous medium, and (ii) on the measurements and validation of light distribution into the greenhouse volume, including the plant stands.

5.2. Towards the development of virtual plants under CFD model

With the recent advances in computing capacities, and to reach more realism with the CFD simulation of the plants, connections should be established with virtual plants that simulate their real activities, meaning indeed a reinforcement of collaborations between greenhouse systems modelers and the physiologists community.

This should integrate in a fine way the functioning of the plant by introducing more accurate mechanisms through the 3D construction of the plants. In such approach, photosynthesis and transpiration will be calculated at the leaf level in the plant architecture according to its microclimate by a transport-resistance system based on the sources/sinks of the various organs. As already seen (Bouhoun Ali et al., 2017), plant water and nutrient uptake can also be included in these augmented reality models (Kim et al. 2021a; 2021b).

5.3. Integration of other biotic/non-biotic interferences

Plants are not the only biotic agents interfering with microclimate in greenhouses, thus fungi, various diseases and insects also directly depend on it and several CFD approaches have recently been performed towards this global integration. Hence, Boulard et al. (2010) have developed and validated a CFD prediction of climate, crop activity and fungal spore transfer in a rose greenhouse, thus showing that both the plants and the airborne transfers of most pathogens can be catch by this approach. Fatnassi et al. (2022) have developed a CFD modelling of the microclimate within the boundary layer of leaves in the ecological niche of most bio-aggressor's and defender's (insects but also fungi and bacteria) to improve pest control management and define how to turn them unfavourably or favourably. Liu et al. (2021) have developed a CFD based 3-D simulation of leaf condensation on cucumber canopy in a solar greenhouse serving as a reference for an early warning model of diseases based on the temporal and spatial distribution of leaf condensation. Their model may serve as a reference for an early warning model of disease based on the temporal and spatial distribution of leaf condensation given that it would be costly to monitor the condensation of all the leaves in a greenhouse. Discrepancies with experimental condensation measurements still exist and further developments are required to improve the model. Furthermore, it will be necessary to cope with the high computational load required by the model to reach the application of this tool in real-time in greenhouse production in the next future, which is of great significance for providing disease warning and guidance in pest control decision-making.

6. Conclusions

A description of the different steps of integrating the greenhouse plant activity in CFD models has been detailed in this paper and particularly the sub-program allowing to calculate the involved parameters as well as the links connecting them with the main solver.

Since the 90s, many CFD models coupling the dynamic effects and mass exchanges between crop and air inside the greenhouse have been developed. Their systematic validations show that they predict accurately the distribution of air speed, temperature, humidity and CO_2 fields inside the greenhouse and the crop rows or canopy. In addition, they provide very important information on plant activity, often including transpiration and more seldom photosynthesis and allow to test improvements of the design and equipment of the greenhouse with respect to crop production.

In a context of resources scarcity such as water and energy, this approach undoubtedly provides comprehensive and easy-to-use tools to tune and optimise the greenhouse system to increase the yield and quality with a low environmental impact.

Appendix A

A.1 Aerodynamic resistance

Within the limits of the climatic variations encountered in greenhouses, the aerodynamic resistance value (r_a) is not very much influenced by the variations in the characteristics of the humid air but depends widely on the air flow regime. Due to the low values of air speed met in greenhouses generally encountered, Baille et al. (1994) considered a constant value of r_a for roses. Nevertheless, several formulas based on local air speed are proposed in the literature (Roy and Boulard, 2005). For greenhouse tomato crops and low wind speeds Boulard et al. (2002) applied the following formulation:

$$r_a = \frac{\rho_a \ C_p}{h_s} \quad \text{(A.1)}$$

where the heat exchange coefficient h_s, depends on the Nusselt number (Nu) and the flow regime near the leaves.

$$h_s = \frac{Nu.\lambda_a}{d} \quad \text{(A.2)}$$

where λ_a is air conductivity (W m^{-1} K^{-1}); d (m) characteristic dimension of the leaves.

Generally, the flow regime near the leaves is widely considered laminar, although it is turbulent further away from leaves and for a laminar flow, Nu can then be written as a function of the convection mode. Assimilating the leaf to a horizontal flat plate (Monteith and Unsworth, 2013; Morille et al., 2013; Roy et al., 2002), the Nusselt number may be expressed as follows according to the convection regime:

Free convection:

$$Nu = 0.59\ (Prt\ .\ Gr)^{0.25} \quad \text{(A.3)}$$

Mixed convection:

$$Nu = 0.68\ (Re^{1.5} + Prt^{0.75})^{0.33} \quad \text{(A.4)}$$

916 Forced convection:

917 $$Nu = \ 0.67\ Re^{0.5}\ Prt^{0.33} \quad \text{(A.5)}$$

918 where Re is Reynolds number; Gr is Grashof number and *Prt* Prandtl number equal to
919 0.71 for air.

920 In the case of a greenhouse without mechanical ventilation, generally free convection
921 prevails inside the greenhouse, and it follows that:

922 $$r_a = \frac{\rho\ C_P d}{0.59\ (\mathrm{Pr}.Gr)^{0.25}\lambda_a} \quad \text{(A.6)}$$

923 **A.2 Leaf stomatal resistance**

924 The leaf stomatal resistance tunes the water vapour transfers through the leaf stomata (Fig.
925 3), the opening stomata driving the transfer of water vapour between the inside of the leaf
926 (where water vapour is saturating) and the surrounding air at leaf surface. They, thus,
927 provide an additional resistance in serial with aerodynamic resistance.

928 Jarvis (1976) has proposed a multiplicative model of stomatal resistance integrating the
929 influence of the different climatic variables on r_s (global radiation R_g, air vapor pressure
930 deficit VPD_a, leaf temperature T_l, concentration of CO_2 in the air C_a). He also assumed that
931 each variable acts independently.

932 $$r_s = r_{smin} f_1(R_g) \cdot f_2(VPD_a) \cdot f_3(T_l).\, f_4(C_a) \quad \text{(A.7)}$$

933 where the $f_\mathbf{i}$ are empirical functions of the different variables studied. He also proposed
934 empirical functions that take the following forms: $f_1(R_g)$ is an asymptotic function (Table
935 A1), $f_2(VPD_a)$ a linear function, $f_3(T_l)$ a hyperbolic function of the leaf temperature T_l,
936 $f_4(C_a)$ a partially linear decreasing function of the CO_2 concentration C_a.

937 Further improvements on Jarvis' model have been proposed by other researchers such as
938 Baille et al. (1994) to model the stomatal resistance of Impatiens who considered that for

939 the case of well-watered plants, the variables that most influence the functioning of the
940 stomata are the incident global radiation (R_g) and air-air vapor pressure deficit VPD_a.

941

942 **Table A1.** The asymptotic function $f_1(R_g)$ for different crops

Formula	Crop	Author
$f_1(R_g) = 1 + \left[exp\left(a_1 \cdot \left(R_g - b_1\right)\right)\right]^{-1}$	tobacco	Avissar et al, 1985
	tomato	Boulard et al., 1991
	banana	Demrati, 2007
$f_1(R_g) = 1 + \frac{a_1}{\left(R_g - b_1\right) \cdot c_1}$	tomato	Stanghellini, 1987
$f_1(R_g) = \frac{1 + a_1 \cdot R_g}{1 + b_1 \cdot R_g}$	not given	Farquhard, 1978
$f_1(R_g) = \frac{a_1 + R_g}{b_1 + R_g}$	9 ornamental species	Baille, 1994

943

944 where a_1, b_1 are parameters determined empirically from data collected in agricultural
945 greenhouse.

946 For VPD_a, Baille et al. (1994) established the following mathematical expression:

947 $$f_2(VPD_a) = 1 + \mathrm{a}_2(VPD_a - VPD_0)^2 \quad \text{(A.8)}$$

948 where VPD_0 is the pressure deficit for which r_s is minimal.

949 For tomatoes another form has been proposed by Boulard et al. (1991) for VPD_a and T_a:

950 $$f_2(VPD_a) = 1 + \mathrm{a}_2 \exp\left(\mathrm{b}_2(VPD_a - VPD_0)\right) \quad \text{(A.9)}$$

951 $$f_2(T_a) = 1 + \mathrm{a}_3 \exp\left(\mathrm{b}_3(T_a - T_{max})\right) \quad \text{(A.10)}$$

where a_2, a_3 and b_2, b_3 , VPD_0 and T_{max} are also empirically determined parameters.

Other authors: Van Bavel (1978); Bot (1983) ; Kimball (1986); Stanghellini (1987); Jolliet et Bailey (1994), have also proposed relationships giving the stomatal resistance as a function of solar radiation and water vapor pressure.

In the case of water restriction, the water state of the soil or the plant becomes a limiting factor for closing or opening of the stomata. Nikolov et al. (1995) and Gang et al. (2012) add a stress function depending on the water potential of the soil and leaf:

$$r_s = r_{smin}\, f_1(R_g)\, f_2(VPD_a)\, f_5(\Psi_s) \qquad \text{(A.11)}$$

$$\text{or } r_s = r_{smin}\, f_1(R_g)\, f_2(VPD_a) f_5(\Psi_l) \qquad \text{(A.12)}$$

References

Acock, B., Charles-Edwards, D. A., Fitter, D. J., Hand, D. W., Ludwig, L. J., Warren-Wilson, J. & Withers, A. C. (1978). The contribution of leaves from different levels within a tomato crop to canopy net photosynthesis: An experimental examination of two canopy models. *Journal of Experimental Botany*, 29, 815-27.

An C.H., Ri H. J., HanT.U., Kim S.I., Ju U.S. (2022). Feasibility of winter cultivation of fruit vegetables in a solar greenhouse in temperate zone; experimental and numerical study. *Solar Energy*, 233, 18-30.

Ansys-Fluent. (2010). Fluent V. 12.1. User's guide.

Avissar, R., Avissar P., Mahrer Y., and Bravdo B. (1985). A model to simulate response of plant stomata to environmental conditions. *Agricultural and Forest Meteorology*, 64, 127–148.

Baille, M., Baille, A., Delmon, D. (1994a). Microclimate and transpiration of greenhouse rose crops. *Agricultural and Forest Meteorology, 71*, 83–97. doi:10.1016/0168-1923(94)90101-5

Baille, M., Baille, A., Laury, J.C. (1994b). A simplified model for predicting evapotranspiration rate of 9 ornamental species vs climate factor and leaf area. *Sci. Hortic. Amsterdam* 59, 217-232.

Bartzanas, T., Boulard, T. and Kittas, C. (2002). Numerical simulation of airflow and temperature patterns in a greenhouse equipped with insect-proof screen. *Computers and Electronics in Agriculture*, 34: 207 - 221.

Bartzanas, T., Boulard, T., & Kittas, C. (2004). Effect of Vent Arrangement on Windward Ventilation of a Tunnel Greenhouse. *Biosystems Engineering*, 88(4), 479‑490. https://doi.org/10.1016/j.biosystemseng.2003.10.006

Baxevanou, C., Fidaros, D., Katsoulas, N., Mekeridis, E., Varlamis, C., Zachariadis, A., & Logothetidis, S. (2020). Simulation of Radiation and Crop Activity in a Greenhouse Covered with Semitransparent Organic Photovoltaics. *Applied Sciences*, 10(7), 2550. https://doi.org/10.3390/app10072550

Ben Amara, H., Bouadila, S., Fatnassi, H., Müslüm A., Guizani A. A. (2021). Climate assessment of greenhouse equipped with south-oriented PV roofs: An experimental and computational fluid dynamics study. *Sustainable Energy Technologies and Assessments*, 45, 2021, 101100, ISSN 2213-1388, https://doi.org/10.1016/j.seta.2021.101100.

Bell, B. (2003). Application Brief: Film Condensation of Water Vapor. Lebanon, New Hampshire, USA: Fluent, Inc.

Bird, R.B., W.E. Stewart, and Lightfoot, E.N. (1960). Transport Phenomena, New York: John Wiley & Sons.

Bot, G.P.A. 1983. Greenhouse climate: from physiqual processes to dynamic model. *Ph. D. Thesis, Agricultural University, Wageningen*, 240 pp.

Bouhoun Ali, H., Bournet, P.E., Danjou, V., Morille, B., Migeon, C. (2014). CFD simulations of the night-time condensation inside a closed glasshouse: Sensitivity analysis to outside external conditions, heating and glass properties. *Biosystems Engineering*, 127, 2014, 159-175, https://doi.org/10.1016/j.biosystemseng.2014.08.017.

Bouhoun Ali, H., Bournet, P.E., Cannavo, P., & Chantoiseau, E. (2017). Development of a CFD crop submodel for simulating microclimate and transpiration of ornamental plants grown in a greenhouse under water restriction. *Computers and Electronics in Agriculture*, https://doi.org/10.1016/j.compag.2017.06.021

Bouhoun Ali, H., Bournet, P.-E., Cannavo, P., & Chantoiseau, E. (2018). Development of a CFD crop submodel for simulating microclimate and transpiration of ornamental plants grown in a greenhouse under water restriction. *Computers and Electronics in Agriculture*, 149, 26‑40. https://doi.org/10.1016/j.compag.2017.06.021

Bouhoun Ali, H., Bournet, P.-E., Cannavo, P., & Chantoiseau, E. (2019). Using CFD to improve the irrigation strategy for growing ornamental plants inside a greenhouse. *Biosystems Engineering*, 186, 130–145. doi.org/10.1016/j.biosystemseng.2019.06.021

Boulard, T., Kittas, C., Roy J.C., Wang, S. (2002). Convective and ventilation transfers in greenhouses, Part 2: Determination of the distributed climate. *Biosystem Engineering* 83 (2), 129-147.

Boulard T., Roy, J.C., Fatnassi, H., Kichah, A., Lee, I-B. (2010). Computer Fluid Dynamics prediction of climate and fungal spore transfer in a rose greenhouse. *Computers and Electronics in Agriculture,* 74, 280-292.

Boulard, T., Baille, A., Mermier, M., Vilette, F. (1991). Mesures et modélisation de la résistance stomatique foliaire et de la transpiration d'un couvert de tomate de serre. *Agronomie,* 11, 259-274.

Boulard, T., Mermier, M., Fargues, J., Smits, N., Rougier, M., Roy, J.C. (2002). Tomato leaf boundary layer climate: implications for microbiological whitefly control in greenhouses. *Agricultural and Forest Meteorology*, 110, 159–176. doi:10.1016/S0168-1923(01)00292-1

Boulard, T., Roy, J.C., Pouillard, J.B., Fatnassi, H., Grisey, A. (2017). Modelling of micrometeorology, canopy transpiration and photosynthesis in a closed greenhouse using computational fluid dynamics. *Biosystems Engineering*, 158: 110 – 133.

Boulard, T., Wang, S. (2002). Experimental and numerical studies on the heterogeneity of crop transpiration in a plastic tunnel. *Computers and Electronics in Agriculture*, 34, 173–190. doi:10.1016/S0168-1699(01)00186-7.

Bournet, P.E., Morille, B., Migeon, C. (2017). CFD prediction of the daytime climate evolution inside a greenhouse taking account of the crop interaction, sun path and ground conduction. *Acta Horticulturae*, 1170, 61–70. https://doi.org/10.17660/ActaHortic.2017.1170.6.

Brown, K.W., and W. Covey. (1966). The energy-budget evaluation of the micro-meteorological transfer processes within a cornfield. Agricultural Meteorology, 3:73–96.

Bruse, M. (1995). Development of a micro-scale model for the calculation of surface temperature in structured terrain. MSc thesis. Bochum, Germany: University of Bochum, Institute for Geography.

Cannavo, P., Bouhoun Ali, H., Chantoiseau, E., Migeon, C., Charpentier, S., Bournet, P.E. (2016). Stomatal resistance of New Guinea Impatiens pot plants. Part 2: Model extension for water restriction and application to irrigation scheduling. *Biosystems Engineering*, 149, 82-93, doi:10.1016/j.biosystemseng.2016.07.001.

CFD2000 manual (v3.0). (1997). Computational fluid dynamics systems. Pacific Sierra Research Corporation, USA.

Chen, J., Xu, F., Tan, D., Shen, Z., Zhang, L., Ai, Q. (2015). A control method for agricultural greenhouses heating based on computational fluid dynamics and energy prediction model. *Applied Energy* 141, 106–118. https://doi.org/10.1016/j.apenergy.2014.12.026

Cheng, X., Li, D., Shao, L., & Ren, Z. (2021). A virtual sensor simulation system of a flower greenhouse coupled with a new temperature microclimate model using three-dimensional CFD. *Computers and Electronics in Agriculture*, 181, 105934. doi:10.1016/j.compag.2020.105934

Defraeye, T., Derome D., Verboven P., Carmeliet J., Nicolai B. (2014). Cross-scale modelling of transpiration from stomata via the leaf boundary layer. *Annals of Botany*, 114(4):711-23, doi:10.1093/aob/mct313.

Demrati, H., Boulard, T., Fatnassi, H., Bekkaoui, A., Majdoubi, H., Elattir, H., Bouirden, L. (2007). Microclimate and transpiration of a greenhouse banana crop. *Biosystems Engineering*, 98, 66-78.

Farquhar, G. D. (1978). Feedforward responses of stomata to humidity. *Australian Journal of Plant Physiology*, 5, 787– 800.

Fatnassi, H., Boulard, T., & Bouirden, L. (2003). Simulation of climatic conditions in full-scale greenhouse fitted with insect-proof screens. *Agricultural and Forest Meteorology*, 118(1‐2), 97‐111. https://doi.org/10.1016/S0168-1923(03)00071-6

Fatnassi, H., Boulard, T., Benamara H., Roy, J.C., Suay, R., Poncet, C. (2016). Increasing the height and multiplying the number of spans of greenhouse: How far can we go? *Acta Horticulturae*, 1170, 137-144, https://doi.org/10.17660/ActaHortic.2017.1170.15

Fatnassi, H., Boulard, T., Poncet, C., & Chave, M. (2006). Optimisation of Greenhouse Insect Screening with Computational Fluid Dynamics. *Biosystems Engineering*, 93(3), 301‐312. https://doi.org/10.1016/j.biosystemseng.2005.11.014

Fatnassi, H., Poncet, C., Bazzano, M. M., Brun, R., Bertin, N. (2015). A numerical simulation of the photovoltaic greenhouse microclimate. *Solar Energy*, 120, 575‐584. https://doi.org/10.1016/j.solener.2015.07.019

Fidaros, D. K., Baxevanou, C. A., Bartzanas, T., & Kittas, C. (2010). Numerical simulation of thermal behavior of a ventilated arc greenhouse during a solar day. *Renewable Energy*, 35(7), 1380‐1386. https://doi.org/10.1016/j.renene.2009.11.013

Gang, L., Yongyi, D., Dongsheng, A., Yongxiu, L., Weihong, L., Xinyou, Y., Chunjiang, Z. (2012). Testing two models for the estimation of leaf stomatal conductance in four greenhouse crops cucumber, chrysanthemum, tulip and lilium. *Agricultural and Forest Meteorology*, 165, 92–103.

Garzoli, K. V. (1985). A simple greenhouse climate model. *Acta Horticulturae*, 174, 393-400.

Goudriaan, J. (1977), Crop Micrometeorology: A Simulation Study, 1st ed., 249 pp., Centre for Agricultural Publishing and Documentation, Wageningen, Netherlands

Green, S. (1992). Modelling turbulent air flow in a stand of widely spaced trees. Phoenics Journal, 5(3), 294–312.

Guyot, G. (1999). In Dunod (Ed.). Climatologie de l'environnement : cours et exercices corrigés (p. 525).

Hang, X., Wang, H., Zou, Z., Wang, S. (2016). CFD and weighted entropy based simulation and optimisation of Chinese Solar Greenhouse temperature distribution, *Biosystems Engineering*, 142, 12-26, https://doi.org/10.1016/j.biosystemseng.2015.11.006.

Haxaire, R. (1999). Caractérisation et Modélisation des écoulements d'air dans une serre. Thèse de Docteur en Sciences de l'Ingénieur de l'Université de Nice, Sophia Antipolis. 148p.

Jarvis (1976) The interpretation of the variations in leaf water potential and stomatal conductance found in canopies in the field. Phil. Trans. R. Soc. Lond. B 273593–610. http://doi.org/10.1098/rstb.1976.0035

Jiao, W., Liu, Q., Lijun, G., Liu, K., Shi, R., Ta, N. (2020). Computational Fluid Dynamics-Based Simulation of Crop Canopy Temperature and Humidity in Double-Film Solar Greenhouse. *Hindawi Journal of Sensors*, Article ID 8874468, 15 pages https://doi.org/10.1155/2020/8874468

Jolliet, O., & Bailey, B. J. (1994). Hortitrans, a model for predecting and optimizing transpiration and humidity in greenhouses. *Journal of Agricultural Engineering Research*, 57, 23-37

Katsoulas, N., Stanghellini, C. (2019). Modelling Crop Transpiration in Greenhouses: Different Models for Different Applications. *Agronomy* 9(7):392.

Kichah, A., Bournet, P.-E., Migeon, C., & Boulard, T. (2012). Measurement and CFD simulation of microclimate characteristics and transpiration of an Impatiens pot plant crop in a greenhouse. *Biosystems Engineering*, 112(1), 22‑34. https://doi.org/10.1016/j.biosystemseng.2012.01.012

Kim, R., Kim, J., Lee, I., Yeo, U., Lee, S., Decano-Valentin, C. (2021a). Development of three-dimensional visualisation technology of the aerodynamic environment in a greenhouse using CFD and VR technology, part 1 : Development of VR a database using CFD. *Biosystems Engineering*, 207, 33‑58. https://doi.org/10.1016/j.biosystemseng.2021.02.017

Kim, R., Kim, J., Lee, I., Yeo, U., Lee, S., Decano-Valentin, C. (2021b). Development of three-dimensional visualisation technology of the aerodynamic environment in a greenhouse using CFD and VR technology, Part 2 : Development of an educational VR simulator. *Biosystems Engineering*, 207, 12‑32. https://doi.org/10.1016/j.biosystemseng.2021.02.018

Kimball, B. A., (1986). A modular energy balance program including subroutines for greenhouses and the other latent devices. U.S.D.A, Agricultural Research Service, ARS-33, 360 pp

Lee, I.B.; Yun, N.K.; Boulard, T.; Roy, J.C.; Lee, S.H.; Kim, G.W.; Lee, S.; Kwon, S.H. (2006). Development of an aerodynamic simulation for studying microclimate of plant canopy in greenhouse-(1) Study on aerodynamic resistance of tomato canopy through wind tunnel experiment. *Journal Bio-Environmental Control*, 15, 289–295.

Lhomme, J.P., Katerji, N. (1991). A simple modelling pf crop water balance for agrometeorological application. *Ecological Modelling*, 57, 11–25

Liu R., Liu J., Liu H, Yang X., Bienvenido Barcena J.F., Li M. (2021). 3-D simulation of leaf condensation on cucumber canopy in a solar greenhouse. *Biosystems Engineering* 210 (2021) 310 -329.

Liu X, Li H, Li Y, Yue X, Tian S. (2020). Effect of internal surface structure of the north wall on Chinese solar greenhouse thermal microclimate based on computational fluid dynamics. *PLOS ONE* 15(4): e0231316. https://doi.org/10.1371/journal.pone.0231316

Majdoubi H., Boulard T., Fatnassi H. and Bouirden L. (2009). Airflow and microclimate patterns in a one-hectare Canary type greenhouse: An experimental and CFD assisted study. *Agricultural and Forest Meteorology* 149, 1050-1062. ISSN 0168-1923, https://doi.org/10.1016/j.agrformet.2009.01.002.

Majdoubi, H., Boulard, T., Fatnassi, H., Senhaji, A., Elbahi, S., Demrati, H., Mouqallid, M., Bouirden, L. (2016). Canary Greenhouse CFD Nocturnal Climate Simulation. Open *J. Fluid Dyn*. 06, 88–100. https://doi.org/10.4236/ojfd.2016.62008 .

Manzoni, S., Katul, G., Fay, P. A., Porporato, A. (2011). Modelling the vegetationeatmosphere carbon dioxide and water vapour interactions along a controlled CO2 gradient. *Ecological Modelling*, 222, 653-665.

Mistriotis, A., Arcidiacono, C., Picuno, P., Bot, G.P.A., Scarascia-Mugnozza, G. (1997a). Computational analysis of ventilation in greenhouses at zero and low-windspeed. *Agricultural and Forest Meteorology* 88, 121–135.

Mistriotis, A., Bot, G.P.A., Picuno, P., Scarascia-Mugnozza, G. (1997b). Analysis of the efficiency of greenhouse ventilation using computational fluid dynamics. Journal of *Agricultural Engineering Research* 85, 217–228.

Mistriotis, A., De Jong, T., Wagemans, M.J.M., Bot, G.P.A. (1997c). Computational fluid dynamics CFD as a tool for the analysis of ventilation and indoor microclimate in agricultural buildings. *Netherlands Journal of Agricultural Science* 45, 81–96.

Molina-Aiz F.D., Fatnassi H., Boulard T., Roy J.C., Valera D.L. (2010). Comparison of finite element and finite volume methods for simulation of natural ventilation in greenhouses. *Computers and Electronics in Agriculture* 72 (2010) 69–86.

Molina-Aiz, F. D., Valera D. L., Alvarez A. J., and Madueno A. (2006). A wind tunnel study of airflow through horticultural crops: Determination of the drag coefficient. *Biosystems Engineering*, 93(4): 447-457.

Molina-Aiz, F.D., Norton, T., López, A., Reyes-Rosas, A., Moreno, M.A., Marín, P., Espinoza, K. and Valera, D.L. (2017). Using Computational Fluid Dynamics to analyse the CO2 transfer in naturally ventilated greenhouses. *Acta Horticulturae,* 1182, 283-292. DOI: 10.17660/ActaHortic.2017.1182.34

Monteith, J., Unsworth, M. (2013). Principles of environmental physics: plants, animals, and the atmosphere. Academic Press

Morille, B., Migeon, C., Bournet, P.E. (2013). Is the Penman–Monteith model adapted to predict crop transpiration under greenhouse conditions? Application to a New Guinea Impatiens crop. *Scientia Horticulturae*, 152, 80–91. doi:10.1016/j.scienta.2013.01.010

Nebbali, R., Roy, J.C., Boulard, T. (2012). Dynamic simulation of the distributed radiative and convective climate within a cropped greenhouse. *Renewable Energy* 43, 111–129. doi:10.1016/j.renene.2011.12.003

Nicot, P., Baille A. (1996). Integrated control of Botrytis cinerea on greenhouse tomatoes. Aerial plant surface microbiology, Plenum Press, 1996, 0-306-45382-7.

Nikolov, N.T., Massman, W.J., Schoettle, A.W. (1995). Coupling biochemical and biophysical processes at the leaf level: an equilibrium photosynthesis model for leaves of C3 plants. *Ecological Modelling* 80, 205–235. doi:10.1016/0304-3800(94)00072-P

Norton, T., Sun, D, Grant, J. Fallon, R., Dodd, V. (2007). Applications of computational fluid dynamics (CFD) in the modelling and design of ventilation systems in the agricultural industry: A review. *Bioresource Technology*, 98, 2386–2414

Okushima, L., Sase, S., Nara, M. (1989). A support system for natural ventilation design of greenhouse based on computational aerodynamics. *Acta Horticulturae* 248, 129–136.

Piscia, D., Montero, J.I., Baeza, E., Bailey, B.J. (2012). A CFD greenhouse night-time condensation model. *Biosystems Engineering*, 111(2), 141-154.

Pouillard, J.B., Boulard, T., Fatnassi, H., Grisey, A., Roy, J.C., (2012). Preliminary experimental and CFD results on airflow and microclimate patterns in a closed greenhouse. *Acta Horticulturae*, 952, 191-198 DOI: 10.17660/ActaHortic.2012.952.23

Reichrath S., Davies T.W. (2001). CFD modelling of the Internal Environment of commercial multi-span venlo-type glasshouses. Paper number 014054, 2001 *ASAE Annual Meeting,* doi: 10.13031/2013.4276

Roy J.C., Boulard T. (2003). CFD predictions of natural ventilation and climate in a tunnel type greenhouse using a transpiration active crop model. *Acta Horticulturae*, 691, 457-464, https://doi.org/10.17660/ActaHortic.2005.691.55

Roy J.C., Boulard, T. (2005). CFD prediction of the natural ventilation in a tunnel-type greenhouse: influence of wind direction and sensibility to turbulence models. *Acta Horticulturae*, 457–464. doi:10.17660/ActaHortic.2005.691.55

Roy, J.C., Boulard, T., Kittas, C., Wang, S. (2002). PA—Precision Agriculture. Biosyst. Eng. 83, 1–20. doi:10.1006/bioe.2002.0107

Roy, J.C., Pouillard, J.B., Boulard, T., Fatnassi, H. and Grisey, A. (2014). Experimental and CFD results on the CO2 distribution in a semi closed greenhouse. *Acta Horticulturae*, 1037, 993-1000 DOI: 10.17660/ActaHortic.2014.1037.131

Roy, J.-C., Vidal, C., Fargues, J., Boulard, T. (2008). CFD based determination of temperature and humidity at leaf surface. *Computers and Electronics in Agriculture*, (61) 201-212

Sase, S., Kacira, M., Boulard, T., Okushima, L. (2012). Wind tunnel measurement of aerodynamic properties of a tomato canopy. *Transactions of the ASABE*, 55(5): 1921-1927

Stanghellini, C. (1987). Transpiration of greenhouse crops. An aid to climate management. PhD Thesis, Agricultural University, Wageningen.

Tadj, N., Nahal, M.A., Draoui, B. and Kittas, C. (2017). CFD simulation of heating greenhouse using a perforated polyethylene ducts. *International Journal of Engineering Systems Modelling and Simulation*, 9(1), 3–11.

Tamimi, E. A., Kacira, M., Choi, C., An, L. (2013). Analysis of microclimate uniformity in a naturally vented greenhouse with a high-pressure fogging system. *Transactions of the ASABE.* 56(3):1241-1254. DOI: 10.13031/trans.56.9985

Thom, A.S. (1971). Momentum absorption by vegetation. *Qtly J. Royal Meteorol. Soc.* 97(414): 414-428.

Thornley, J.H.M. (1976). Mathematical models in plant physiology. Academic press, London

Tong, G., Christopher, D.M., Li, B. (2009). Numerical modelling of temperature variations in a Chinese solar greenhouse. *Computers and Electronics in Agriculture,* 68 (1), 129–139

Tong, G., Christopher, D.M., Zhang, G. (2018). New insights on span selection for Chinese solar greenhouses using CFD analyses. *Computers and Electronics in Agriculture*, Volume 149, 2018, Pages 3-15, https://doi.org/10.1016/j.compag.2017.09.031.

Van Bavel, C. H. M., Lascano R., Wil-son. D.R. (1978). Water relations of fritted clay. *SoilSci. Soc. Amer. J.* 42:657-659.

Van Bavel, C. H. M., Takakura, T., Bot, G. P. A. (1985). Global comparison of the greenhouse climate models. *Acta Horticulturae*, 174, 21-33.

Wang, X.W., . Luo, J.Y., Li X.P. (2013). CFD Based Study of Heterogeneous Microclimate in a Typical Chinese Greenhouse in Central China. *Journal of Integrative Agriculture*, 12(5), 914-923, https://doi.org/10.1016/S2095-3119(13)60309-3.

Wilson, J.D., (1985) Numerical studies of flow through a windbreak. *J Wind Eng Ind Aerodyn* 21:119–154

Wu X., Liu X., Yue X., Xu H., Li T., and Li Y. (2021). Effect of the ridge position ratio on the thermal environment of the Chinese solar greenhouse *R. Soc. open* sci.8201707201707. http://doi.org/10.1098/rsos.201707

Yu, G., Zhang, S., Li, S., Zhang, M., Benli, H., Wang, Y. (2022). Numerical investigation for effects of natural light and ventilation on 3D tomato body heat distribution in a Venlo greenhouse. *Information Processing in Agriculture*, https://doi.org/10.1016/j.inpa.2022.05.006.

Conflict of interest

The authors declare that they have no known competing financial interests or personal relationships that could have appeared to influence the work reported in this paper.

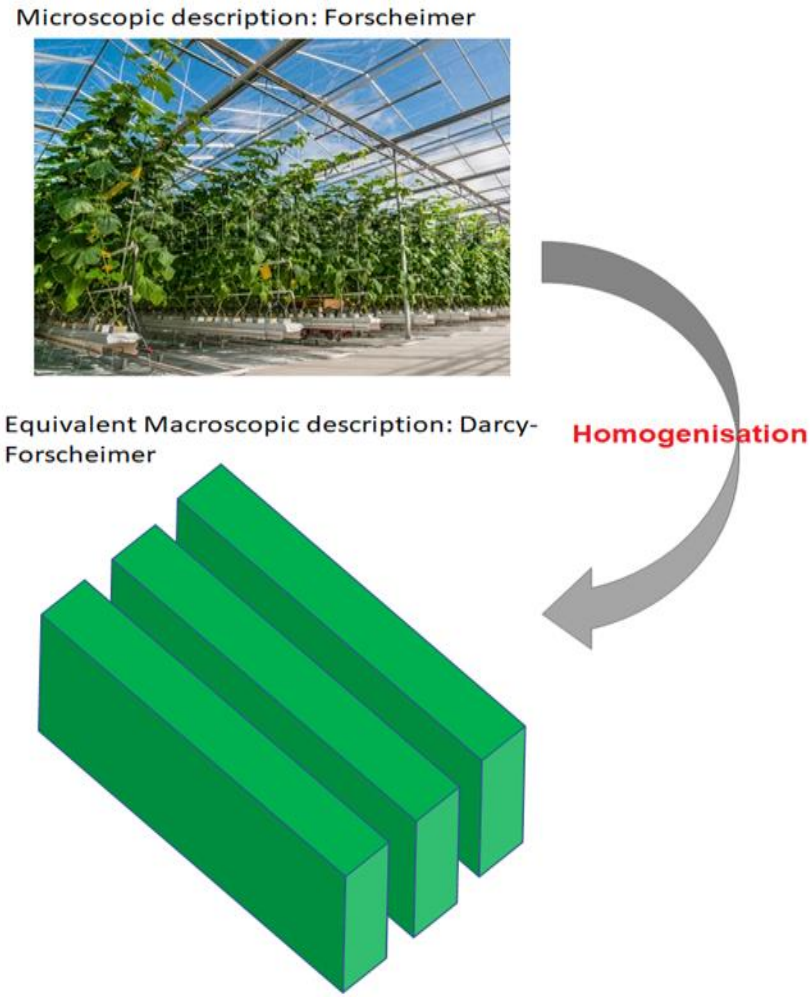

Fig.1 Description of the crop: homogenization method

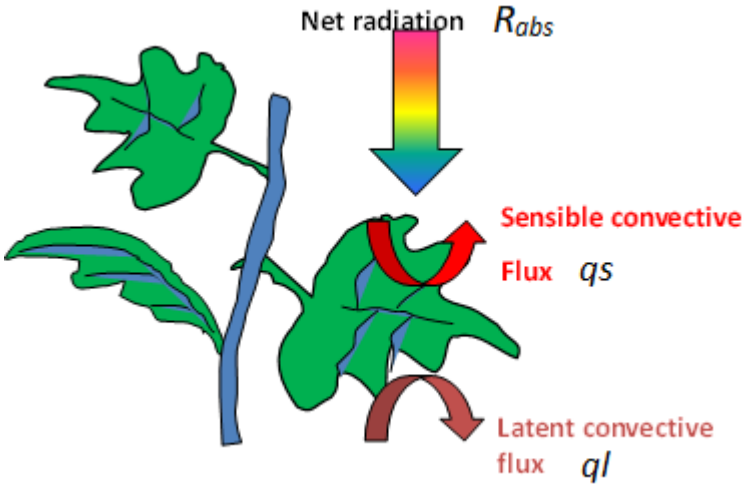

Fig.2 Net radiation, sensible and latent heat balances of leaves

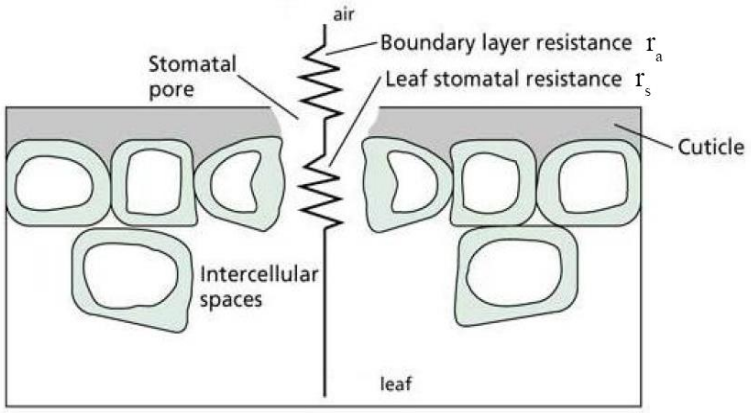

Fig.3 Resistances to water vapor transfer between leaf and air

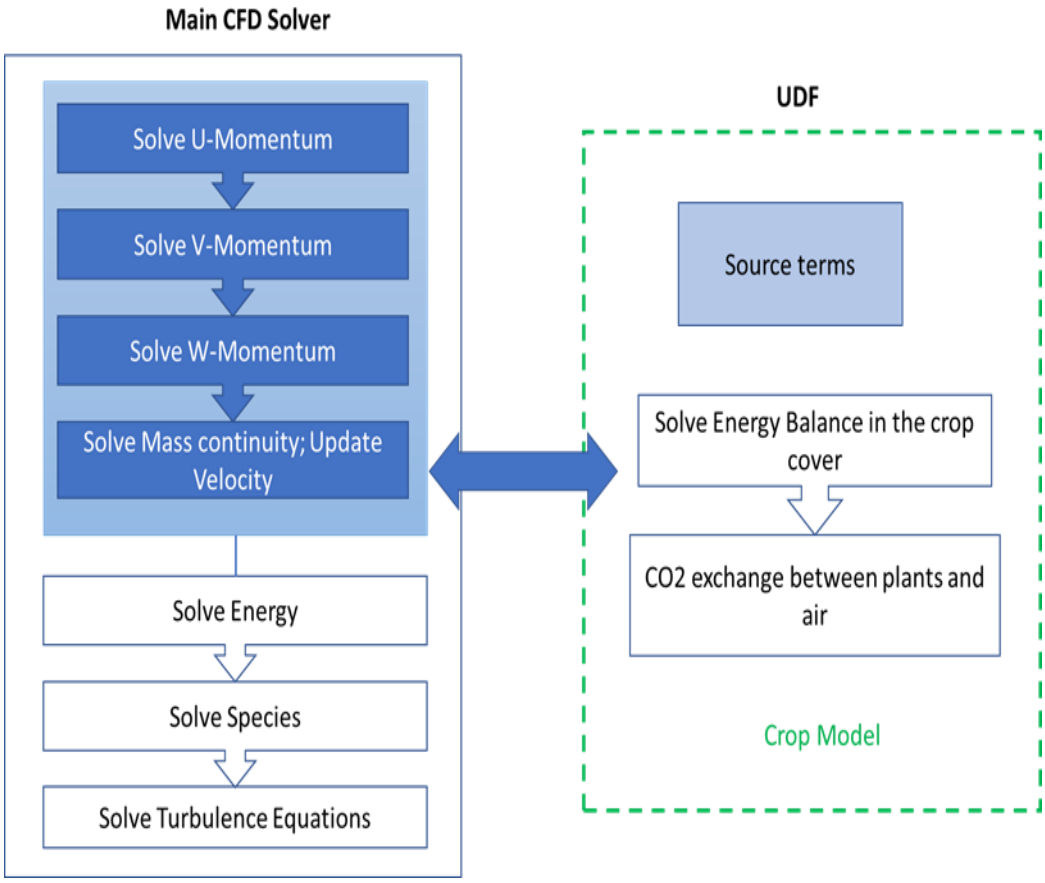

Fig. 4 Sketch of the exchanges between the UDF and the main solver in the CFD model.

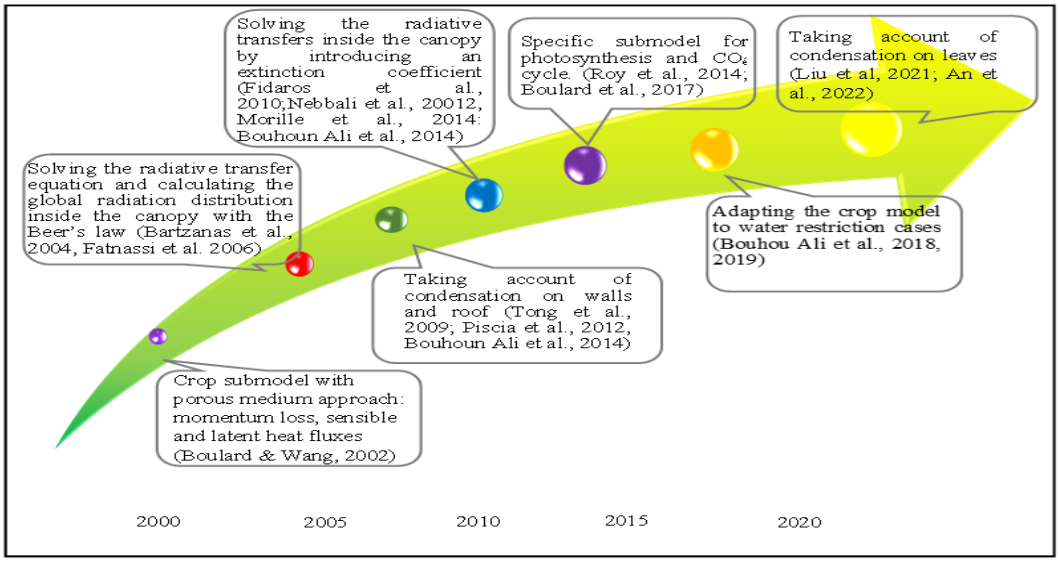

Fig. 5 Milestones of CFD crop submodel developments

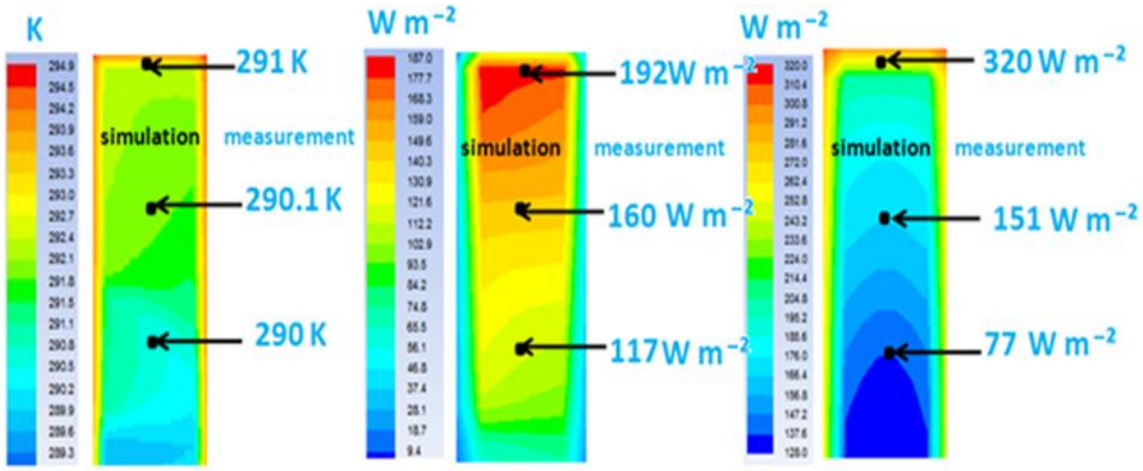

Fig. 6 Simulated and measured distributions of leaf temperature in K (left), latent heat of crop transpiratin in W m^{-2} (middle) and short waves radiations in W m^{-2} (right) within the crop cover at noon (after Pouillard et al., 2012).

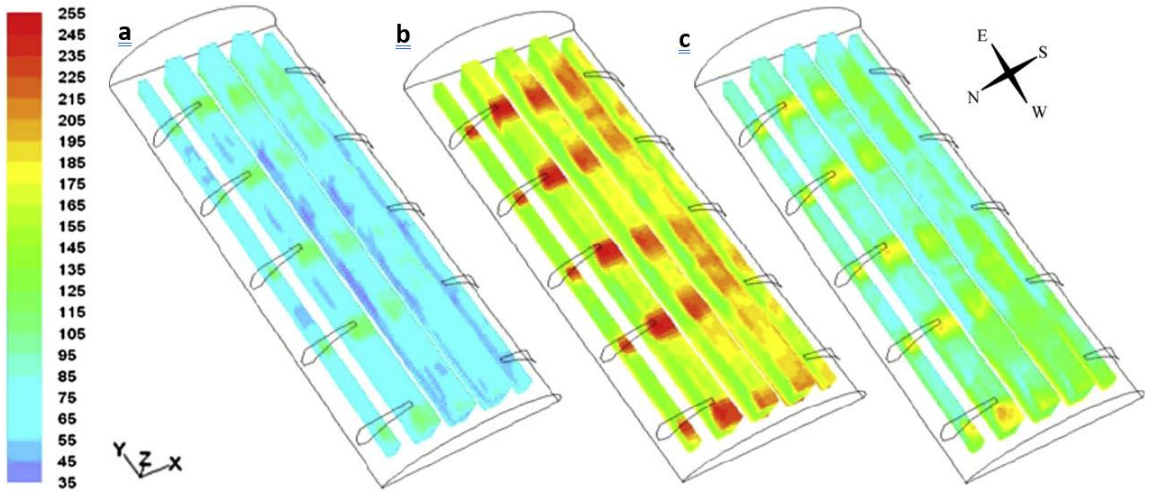

Fig. 7 Distribution of the transpiration heat flux density on June 21st. (a): at sunrise, (b): at midday, (c): at sunset (after Nebbali et al., 2012)

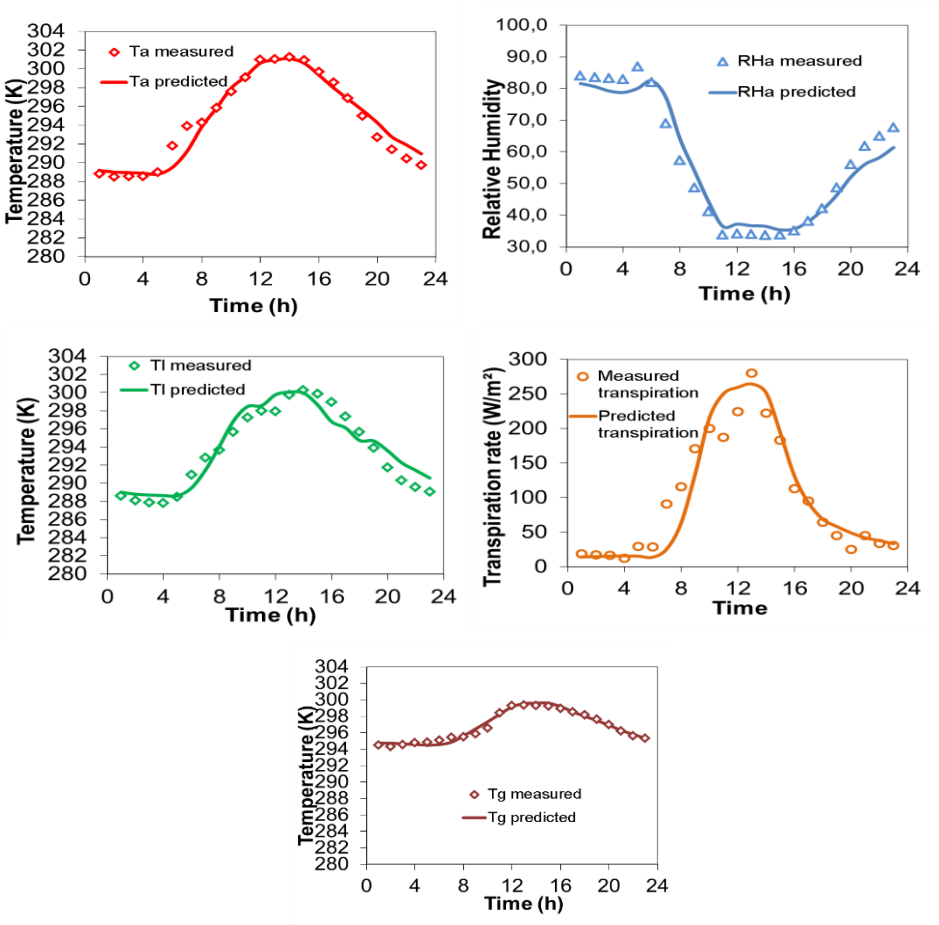

Fig.8 Comparison of measurements and CFD simulations for A) air temperature above the crop; B) relative humidity above the crop; C) leaf temperature, D) transpiration rate and E) soil surface temperature (adapted from Bournet et al., 2017).

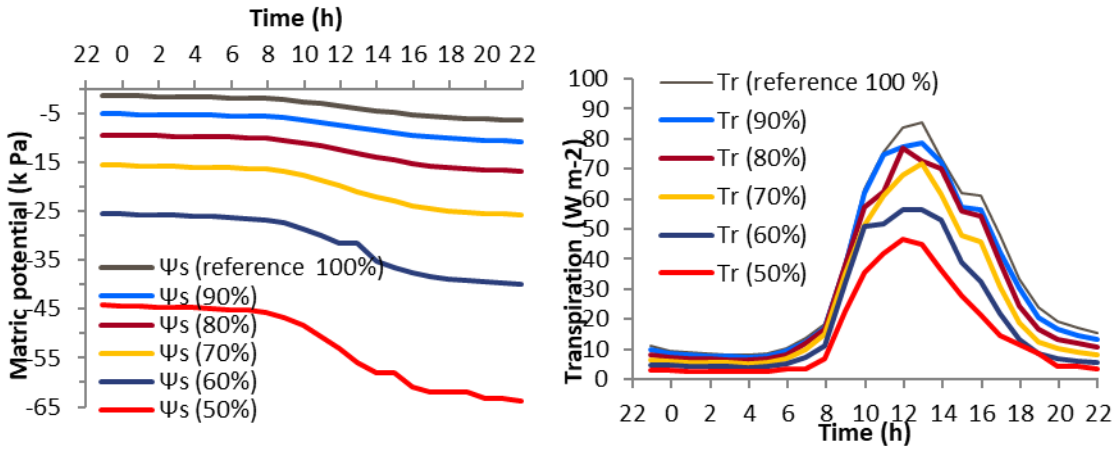

Fig. 9 Evolution of the matric potential in the ground (a) and corresponding evolution of the evapotranspiration predicted by a CFD model for an impatiens crop (b) (after Bouhoun Ali et al., 2018)

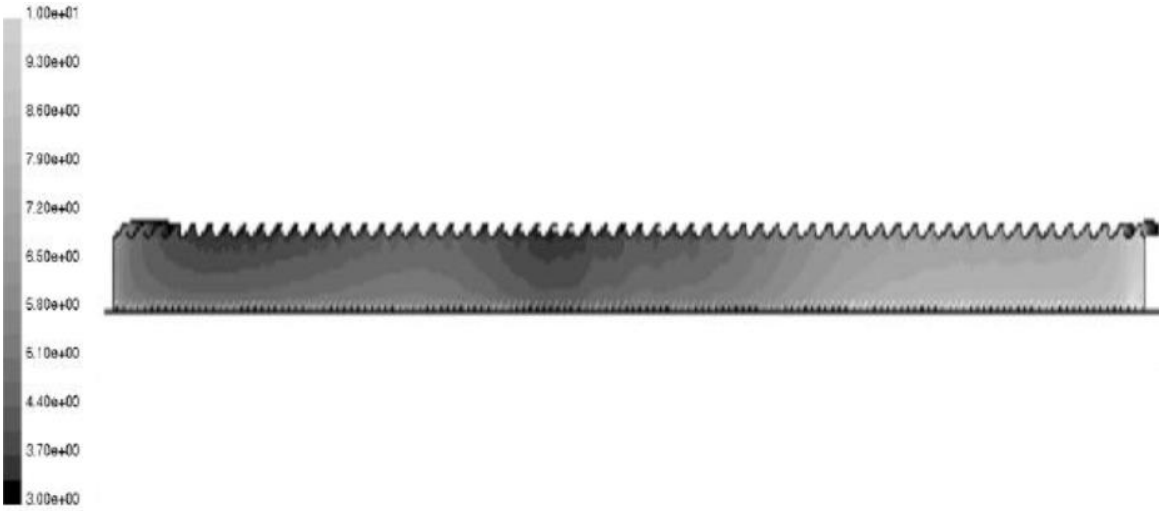

Fig.10 Carbon dioxide dispersion in a 60 span Venlo-type glasshouse with crops (after Reichrath et al., 2001).

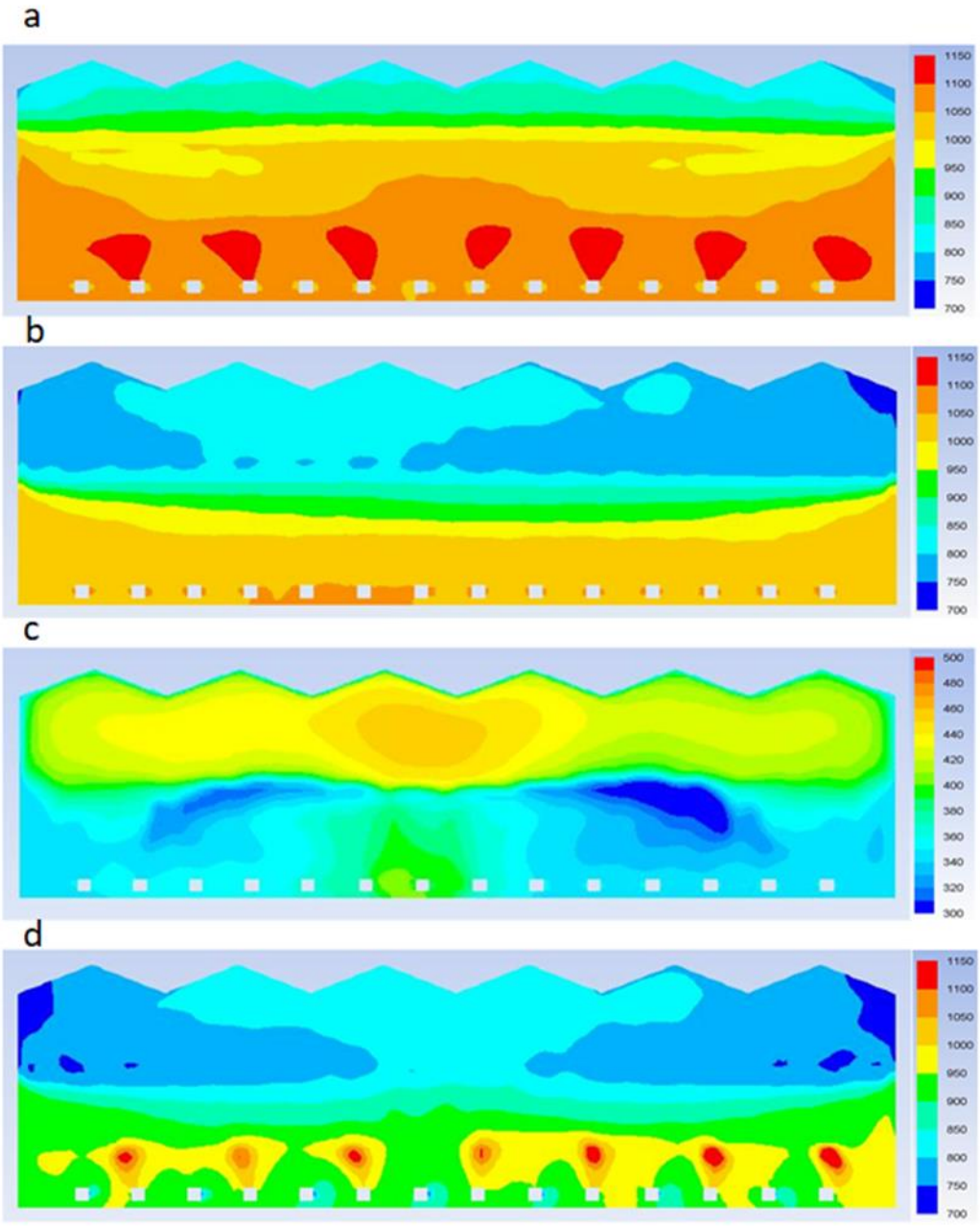

Fig. 11. Simulated carbon dioxide levels (ppm) in a median vertical transverse plane of the greenhouse at (a) 8:00 am; (b) 11:30 am; (c) 1:00 pm; (d) 5:30 pm. (After Boulard et al., 2017).

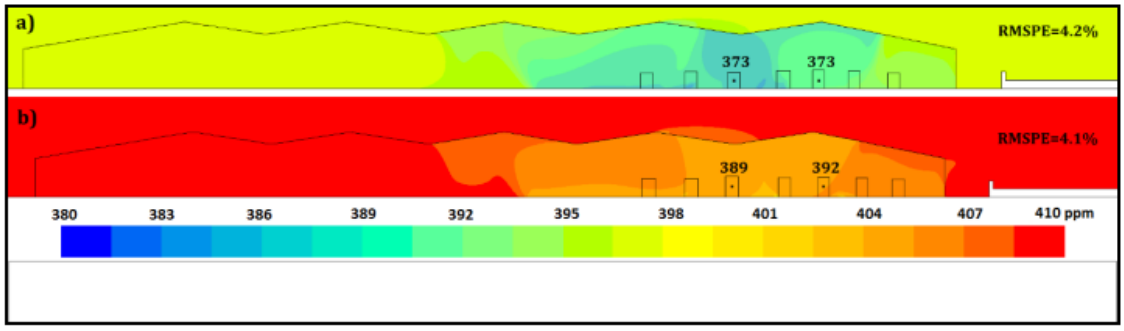

Fig. 12. Distributions of CO_2 concentration simulated with CFD and measured values (indicated in the figures) in the greenhouse on (a) 3/11/2014 and (b) 3/13/2014. (After Molina et al., 2017)

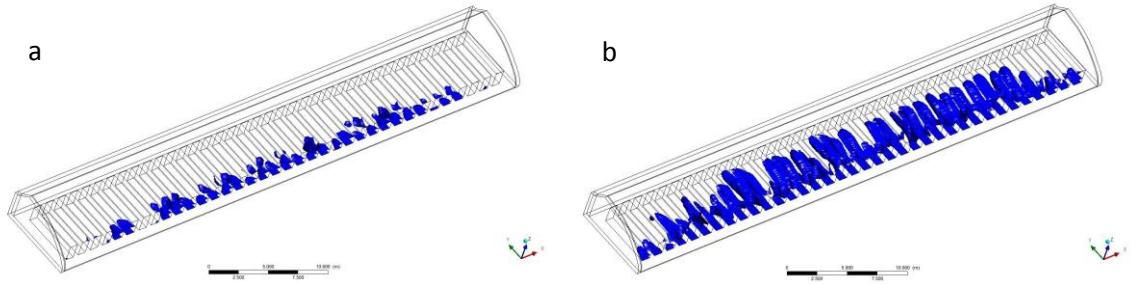

Fig. 13. Simulated leaf condensation on April 17 at (a) 01:30 and (b) 05:30. Y represents the north; X represents the east; and ■ represents the condensation that appeared based on simulation (after Liu et al., 2021).

Table 1. Validation studies of the CFD model based on the comparison between measured and simulated values of climate parameters in the greenhouse

Authors	Greenhouse type	Crop	Dimension	Validation
Boulard & Wang (2002)	Tunnel	Lettuce	3D steady	Transmittance, air velocity Temperature, transpiration flux
Fatnassi et al. (2003)	Moroccan type	Tomato	3D steady	Ventilation rate
Bartzanas et al. (2004)	Tunnel	Tomato	2D/3D steady	Air velocity, ventilation rate, air temperature
Fatnassi et al. (2006)	Multi span	Roses	3D steady	Ventilation rate
Majdoubi et al. (2009)	Canary type	Tomato	3D steady	Air temperature, relative humidity
Tong et al. (2009)	Chinese	Lettuce	2D unsteady	Air temperature
Boulard et al. (2010)	Multispan plastic	Roses	2D unsteady	Air temperature and humidity, spore concentration
Piscia et al. (2012a)	4-span plastic	Lettuce	3D unsteady	Air temperature, roof temperature, humidity ratio
Tamimi et al. (2013)	Arch type	Tomato	3D steady	Air velocity, evapotranspiration, stomatal resistance
Majdoubi et al. (2016)	Canarian	Tomato	3D steady	Air temperature and humidity
Bouhoun Ali et al. (2018)	Venlo glass house	New Guinea Impatiens	2D unsteady	Air temperature, leaf temperature matric potential, stomatal resistance, air humidity, transpiration rate
Boulard et al. (2017)	6-span glasshouse	Tomato	3D unsteady	Air temperature, leaf temperature, saturated humidity at leaf temperature, air humidity, shortwave radiation, air speed, crop transpiration, CO_2 concentration
Bouhoun Ali et al. (2019)	Venlo glass house	New Guinea Impatiens	2D unsteady	Air temperature and humidity, stomatal resistance, ventilation rate
Fatnassi et al. (2021)	Four-span plastic arched greenhouse	Rose	3D unsteady	Air temperature and humidity

Table A1. The asymptotic function $f_1(R_g)$ for different crops

Formula	Crop	Author
$f_1(R_g) = 1 + \left[exp\left(a_1 \cdot (R_g - b_1)\right)\right]^{-1}$	tobacco	Avissar et al, 1985
	tomato	Boulard et al., 1991
	banana	Demrati, 2007
$f_1(R_g) = 1 + \frac{a_1}{(R_g - b_1) \cdot c_1}$	tomato	Stanghellini, 1987
$f_1(R_g) = \frac{1 + a_1 \cdot R_g}{1 + b_1 \cdot R_g}$	not given	Farquhard, 1978
$f_1(R_g) = \frac{a_1 + R_g}{b_1 + R_g}$	9 ornamental species	Baille, 1994

Editorial Office
Academic Editor
Biosystems Engineering Journal

Dear Professor Nikolaos Katsoulas ,

Please find enclosed, the revised version of our manuscript "YBENG-D-22-01328", for publication in Biosystems Engineering Journal, by Hicham Fatnassi et al. entitled "*Use of Computational Fluid Dynamic tools to model the coupling of plant canopy activity and climate in greenhouses and closed plant growth systems: a review"*.

I have carefully considered each comment and made the necessary changes to the text. As you will see from the margin notes, I have addressed all your concerns.

I would like to express my gratitude for the time and effort you and the reviewers have invested in reviewing my manuscript. The comments and suggestions have been invaluable in improving the quality of the manuscript, and I believe that the revised version represents a significant improvement over the original submission.

Sincerely yours,

Hicham Fatnassi and co-authors